Synopsis

A computational investigation has been carried out in the field of charged-particle optics. The work is concerned with the design of electrostatic lenses with and without misalignment effect operated under different magnification conditions.

The potential field distributions of einzel and immersion electrostatic lenses have been represented by analytic functions. The paraxial ray equation has been solved for the proposed fields to determine the trajectory of the charged particles traversing each lens. From the axial potential distribution and its first and second derivatives, the optical properties such as the focal length and spherical and chromatic aberrations have been compute. The electrode shape of each electrostatic lens has been determined in the two-and three-dimensions. The aberration of the electrostatic lens is highly dependent on the alignment of the electrodes and it has been found to be an important parameter affecting the geometry of the electrostatic lens system.

The results of this investigation not only prove in theory the possibility of designing electrostatic lens systems with low aberration but also show the possibility of constructing such lenses in practice.

CONTENTS

3. RESULTS AND DISCUSSION

4. CONCLUSIONS AND RECOMMENDATIONS FOR FUTURE WORK

List of symbols

a, b, c	Constants affecting the voltage ratio (V)
d, e, h	Constants affecting the shift function U_{SL} (mm)
Cc	Chromatic aberration coefficient
Cs	Spherical aberration coefficient
dc	Chromatic aberration disk (mm)
ds	Spherical aberration disk (mm)
dt	Total aberration disk, $dt=(d^2s+d^2c)^{1/2}$ (mm)
$\Delta E/E$	Energy spread
f_i, f_0	Focal lengths in the image and object side respectively
f_{1i}	First harmonic field function for the j^{th} deflector
L	Length of the lens field (mm)
M	Linear magnification
m	Mass of charged particles
p	Momentum of charged particles (kg.m / s)
q	Charge of particles (C)
r	Radial displacement of the beam from the optical axis
r'	Derivative of the radial displacement with respect to z, i.e.dr/dz
s_L, s_D	Lens and deflector axises shift from the optical axis respectively
U=U(z)	The axial potential distribution (V)
U_o	Accelerating voltage (V)
U_1, U_2	Electrode voltages (V)
U', U''	First and second derivatives of axial potential with respect to z, i.e. dU/dz, d^2U/dz^2
U_{SL}	The shift function (mm)
V_x, V_y	x and y directional deflector voltages
x_i	Rotation angle of deflector

z	Optical axis
z_o, z_i	Object and image positions respectively
α	Half acceptance angle of the aperture (mrad)

طالبة الماجستير : رؤى تحسين عبد الله الصميدعي

عنوان الأطروحة :

THE ABERRATION CORRECTION DUE TO MISALIGNMENT IN ELECTROSTATIC LENSES

(تصحيح الزيغ بسبب عدم التراصف في العدسات الكهروسكونية)

المشرف : د.أحمد كمال أحمد

تأريخ المناقشة : ٢٠٠٦\١٠\٥

لجنة المناقشة :

١. د.أياد عبد العزيز العاني
٢. د.محمد عز الدين الصندوق
٣. د.سمير خضر ياسين العاني

1. INTRODUCTION

1.1. Electrostatic Lenses

Any axially symmetric electrostatic field is in fact a lens. Electrostatic fields are produced by sets of electrodes held at suitable potentials; in other words, any axially symmetric electrode system constitutes an electrostatic lens. Electrostatic lenses are finding increasing application in many areas and technology, because of the rapid development of modern instrumentation. Electrostatic lenses have the following most important features **(Szilagyi 1988, Hawkes and Kasper 1989)**:

(a) For the non-relativistic cases the focusing properties as well as the aberrations are independent of the charge-to-mass quotient of particles, therefore electrostatic lenses may be used focusing various ions.

(b) Potential ratio have influence on the lens properties. Therefore, if particles of the opposite sign have to be focused, the signs of all electrode potential must be reversed to arrive at the same properties. The particles trajectory remains the same if both the sign of the particles charge and the electrode potentials are reversed.

(c) Electrostatic lenses are characterized by their simple electrodes fabrication, alignment, small size, and relatively light weight. Furthermore, their low power requirement suggest the need of lighter and more stable power supplies. The major manufacturing problems are electric breakdown and accumulation of charges on the insulating surfaces.

1.2. Type of Electrostatic Lenses

There are various types of electrostatic lenses for different electron and ion optical systems, each with its own optical properties and domain of application. The lenses can be classified from many different points of view, for example, one can talk about (a) strong or weak lenses depending on whether their focal points are situated inside or outside the field, (b) thick or thin lenses, (c) symmetric or asymmetric lenses.

In classical texts of electron optics electrostatic lenses were classified into group according to the relationships between their electrode potentials, figure 1-1 depicts how the plot of the potential $\mathbf{U_o}(z)$ behaves along the z-axis for several kinds of electrostatic lenses. The main groups are **(Szilagyi 1988)**:

(a) The immersion lens, with two different constant potential at the different sides.

(b) The unipotential (einzal) lens, having the same constant potential at both the object and image sides.

(c) The cathode lens, having a field abruptly terminated on the object side by the source of the charged particles.

(d) The diaphragm (signal-aperture) lens, with a homogeneous field on at least one side.

(e) The foil lens. It consists of thin metal films transparent to the particle and possessing discontinues field distributions.

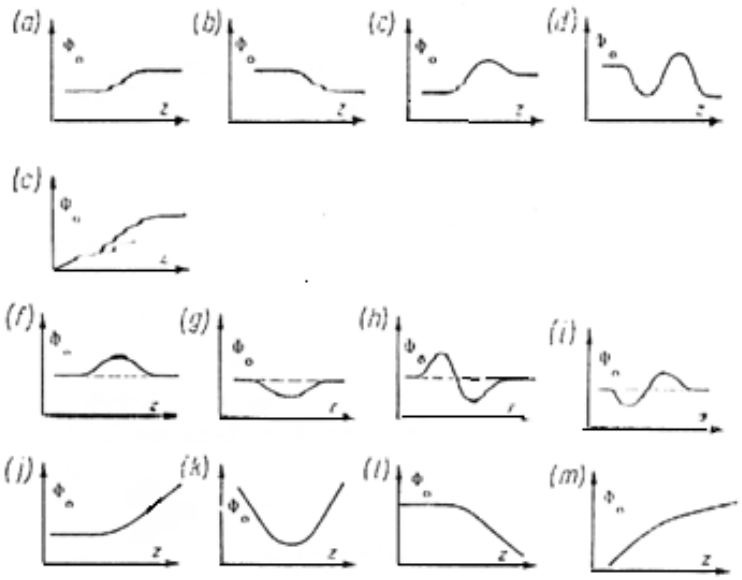

Figure 1-1: Distribution of the axial potential in electrostatic lenses (a) to (d)-immersion lenses; (e)-cathode lens; (f) to (i)-unipotential lenses; and (j) to (m)-diaphragm lenses **(Paszkowski 1968)**.

1.3. Historical Development

The optimization of electron optical element is a problem which is easy to formulate but rather difficult to solve **(Szilagyi 1977a)**. Its aims to find such electrostatic field distributions which produce as small aberrations as possible. Several approaches have been proposed by **(Hawkes 1973)**, and **(Munro 1975)**. The calculus of variations was applied successfully by **Moses 1970, 1971**, but its mathematical complexity puts a limit to the practical applications.

Szilagyi (1977a) proposed a simple approach to the optimization problem based on dynamic programming and the linear electron lens models. The first results of

the application of dynamic programming principle to electron optical optimization were presented by **Szilagyi (1977b)**.

Szilagyi (1984) described a computational technique for optimal control problems arising in the synthesis of electron and ion lenses. The method provides an effective search algorithm for electrostatic field with minimum aberrations.

A novel approach to electron/ion optical synthesis and optimization was presented by **Szilagyi (1985)**. Low-aberration field distributions are sought by dynamic programming or optimal control procedures in the form of continuous curves constructed of cubic splines.

Tsumagari (1986) developed an aberration theory for analyzing the effects of machining error of electrostatic ion-optical systems comprising round lenses and octupole deflectors. The relationship has been investigated between the machining error and the induced perturbation.

A thorough investigation of axially symmetric two-electrode electrostatic lenses was presented by **Szilagyi, Szep, and lugosi (1987)**. The study is based on the analysis of axial potential distributions, according to the principle of synthesis.

Glatzel and Lenz (1988) adopted a method which has been successfully applied in light optics, by describing the charged-particle optical system by a finite number of parameters P_k ($_{k=1, \ldots..,m}$). Some of these parameters may be geometrical, i.e. they described the shapes and positions of the electrodes, polepieces and some other operational parameters such as electrode potentials, numbers of amperes-turns or other lens strength parameters.

Szép and Szilagyi (1988) presented a novel approach to the synthesis of axially symmetric electrostatic lenses with minimum aberration. The method uses computer optimization to determine the electrode potentials of a multielectrode lens. The same method can be used for designing lenses for many different applications.

Kiss (1989) discussed a computerized systematic investigation to find axially symmetric electrostatic lens potential with acceptable first-order properties and small spherical aberration. The calculation of the spherical aberration is based on the direct solution of the relativistic trajectory equation in paraxial and nonparaxial approximation.

The aberration of electrostatic lens and electrostatic deflection systems due to misalignment was analyzed by **Kurihara (1990)** for the design of microfabrication system. The potential for lens and deflector having an electrode axis shift was approximated by introducing a shift function that expressed the electrode shift from the optical axis. On the basis of this approximation, mixed aberrations due to misalignment of lens and deflector electrodes can be analyzed, including the effect of a nonuniform electrode axis shift.

The use of the electron beam trajectory as a major parameter for determining the design of electrostatic lens at zero and infinite magnification operational conditions was investigated in detail by **Ahmad (1993**) in the absence of space charge-effect and by **Al-Ani (1996)** in the presence of space charge.

The near-axis aberration for electrostatic systems caused by the presence of a localized potential defect (i. e., a path field) near the edge of an aperture was investigated by **Read (1998)**.

Aberrations for two types of multiplets based on electrostatic quadrupole and octupole lenses: mid-acceleration systems in which an accelerating potential is applied to the middle lenses of a set of quadrupole lenses and systems in which some of the quadrupole lenses are replaced by combined quadrupole-octupole lenses were investigated and compared by **Baranova and Read (1999)**. It is shown that for systems consisting of three lenses the mid-acceleration type has the smaller aberration.

Image aberration resulting from small misalignment in quadrupole lenses multiplets had been analysed by **Baranova and Read (2001)**. Analytical formulas for the coefficients of the beam displacement, astigmatism and coma associated with misalignments in a general quadrupole lens system have been derived.

A computational investigation was carried out by **AL-Mudarris (2001)** in the field of non-relativistic charged-particle optics. The work was concentrated on the simulation of a transport and focusing ion-optical system consisting various types of electrostatic lenses.

Two aspects of the design of electrostatic aberration correctors for low voltage scanning electron microscopes are considered by **Baranova , Read and Cubric (2004)**.The first is that of optimizing the geometry and scale size so that the fields at the surfaces of the electrodes do not exceed the breakdown value. The second aspect is that of providing an accurate computational simulation of the paraxial fields of the lens system.

1.4. Optimization: Analysis and Synthesis

Any reasonable design of an electron or ion optical system must take the aberrations into account. There are two fundamental approaches to optimize the parameters of a charged-particle optical system: (i) the analysis (ii) the synthesis of electron and ion systems **(Szilagyi 1985)**. The optimization approach is searching for such electron and ion optical elements that would provide the required optical properties with minimum aberrations.

The first approach is based on trial and error. The designer starts with given simple sets of electrodes or pole pieces and tries to improve the design by analyzing the optical properties and changing the geometrical dimensions as well as the electric and magnetic parameters of the system. This process must be repeated until it converges to an acceptable solution. Due to the infinite number of possible configurations, the procedure is extremely slow and tedious.

In the second approach, the word synthesis which is sometimes called inverse problem of charged-particle optics, i.e. for finding field distribution that would produce given trajectories **(Szilagyi 1988)**. This approach is based on the fact that for any imaging field, its optical properties and aberrations are totally determined by the axial distribution of the field.

Only the axial distributions and their derivatives appear in those expressions. Then, instead of analyzing a hopelessly vast amount of different electrode and pole piece configurations we can take the criteria defining an optimum system as initial conditions and try to find the imaging field distribution (and hence synthesis the electrodes or pole pieces) that would produce it. i.e. in synthesis approach, one try to find the best axial field distribution or best shapes of these axial distributions that would satisfy the given constraints.

1.5. Aim of the Thesis

The present work aims at finding the design of electrostatic lens with and without misalignment effect, which give rise to the minimum spherical and chromatic aberrations. Synthesis approach of optimization method is used in the present work.

The suggested types of electrostatic lenses are einzel and immersion lens where their electrodes configuration and optical properties are determined from suggested mathematical models representing the potential distribution.

Two of the various magnification conditions that are well-known in electron optics have been taken into account in the present project, namely, the infinite and zero magnification conditions due to their resemblance to the lens trajectory.

The space charge effects are neglected in order to satisfy Laplace's equation $\nabla^2 U = 0$ where ∇^2 is called the Laplacian operator and U is the electrostatic potential (scalar potential) measured in volts. Laplace's equation determined the function U in charge-free regions.

2. THEORETICAL CONSIDERATIONS

2.1. Axially Symmetric Electrostatic Fields

Axially symmetric fields (or rotationally symmetric fields) are of particular interest in electron optics. The most common electron lenses are round, which means that they are built up from rotationally symmetric fields **(Hawkes and Kasper 1989)**.

The most suitable coordinate system to field with rotational symmetry is the cylindrical polar coordinate system. The z-axis is the optical axis which represents the axis of symmetry. The value of the potential at any point can be expressed in terms of the three coordinates z, r and θ i.e. U=U(z,r,θ). The condition for rotational symmetry in cylindrical coordinates can be expressed by U(z,r,θ)=U(z,r), where the values of z and r uniquely define the value of U, regardless of the angle of rotation. In rotationally symmetric space-charge-free fields, Laplace's equation, is reduced to the following form **(Zhigarev 1975)**:

$$\frac{1}{r}\frac{\partial}{\partial r}\left[r\frac{\partial U}{\partial r} \right]+\frac{\partial^2 U}{\partial z^2}=0 \qquad (2\text{-}1)$$

The solution of equation (2-1) can be written in the form of a power series of r as in the following form:

$$U(r,z)=U_o(z)+U_1(z)\,r^2+U_2(z)\,r^4+ \quad \ldots\ldots..$$

$$=\sum_{n=0}^{\infty}U_n(z)r^{2n} \qquad (n=0,1,2,\ldots..) \qquad (2\text{-}2)$$

This series contains only even powers of r, since rotational symmetry implies that U must be an even function, and hence, all odd powers must vanish **(El-Kareh and El-Kareh 1970)**. By differentiating the series twice with respect to z one time and then twice with respect to r, and utilizing it into equation (2-1) an expression

for the potential of rotationally symmetric fields can be obtained **(Zhigarev 1975)**,

$$U(r,z)=\sum_{n=0}^{\infty}\frac{(-1)^n}{(n!)^2}\left[\frac{r}{2}\right]^{2n} U_o{}^{2n}(z)$$

$$=U_0(z)-\frac{r^2}{4}U_0''(z)+\frac{r^4}{64}U_0''''-\ldots\ldots \qquad (2\text{-}3)$$

The first term $U_o(z)$ determines the potential distribution along the axis of the system (r=0), i.e. $U_o(z) = U(0,z)$. The power series expansion allows to calculation of the fields in the entire space provided that the axial potential distribution $U_o(z)$ is known, and this distribution is a function which is differentiable an infinite number of time.

The potential of rotationally symmetric fields due to misalignment effect is approximated by introducing a shift function that expresses the electrode shift from the optical axis, i.e. by substituting r by $r–U_{SL}(z)$ in equation (2-3) results **(Kurihara 1990)**:

$$U(r,z)=U_0(z)-\frac{1}{4}U''_0(z)\left[r-U_{SL}(z)\right]^2+\frac{1}{64}U''''_0\left[r-U_{SL}(z)\right]^4-\ldots\ldots \qquad (2\text{-}4)$$

where $U_{SL}(z)$ is the shift function which has following suggested form :

$$U_{SL}(z)=\tanh\left[\frac{z}{d}\right]-\left[\frac{z}{e}\right]+h \qquad (2\text{-}5)$$

The constants d, e and h effect the properties of this suggested function and have been the following values: d=4mm, e=800mm and h=0.5mm. The values of the constants are suggested to fit for the suggested curve. The constants d, e and h has the units of millimeter to match the unit of $U_{SL}(z)$.

2.2. Paraxial-Ray Equation in Electrostatic Field

The trajectory of electrostatic symmetrical electron or ion optical system is given by the following equation **(Szilagyi 1988)**:

$$r''+\frac{U'}{2U}r'+\frac{U''}{4U}r=0 \qquad (2\text{-}6)$$

where *r* is the radial displacement of the beam from the optical axis z, and the primes denote a derivative with respect to *z*. *U=U(z)* is the electrostatic potential distribution along the optical axis *z*. Equation (2-6) is a linear homogeneous second-order differential equation, known as the paraxial-ray equation which describe the paths of charged particles moving through a roationally symmetrical electrostatic field characterized by the potential function *U*. The paraxial-ray equation was first derived by Busch in 1926. Many imporfant deductions can be made from this equation:

a. The quotient of charge-to-mass (q/m) does not appear in the equation. Therefore, the trajectory is the same for any charged particle eneterning the field with the same initial kinetic energy, but arrive to the same focus at different times.

b. The equation is homogeneous in *U*. Therefore, an equal increase (or decrease) in the potential *U* at all the points of field (multiplying the potential by any constant) does not change the trajectory.

c. The equation is homogeneous in *r* and *z* which indicates that any increase in the dimensions of the whole system produces a corresponding increase in the dimensions of the trajectory, since the equipotentials, though of the same form, are enlarged. If the object is doubled in size, the image will be doubled in size; the ratio between the two remains constant.

The paraxial ray equation including the misalignment effect is given by **(Kurihara 1990)**:

$$r'' + \frac{U'}{2U} r' + \frac{U}{4U} r = -\frac{VF_1(z)}{2U} + \frac{U''}{4U} U_{SL} \qquad (2\text{-}7)$$

where

$$F_1(z) = \sum_{j=1}^{n} f_{1i}(z)\exp(ix_i), \quad (2\text{-}8)$$

and

$$V = V_x + iV_y \quad (2\text{-}9)$$

Here f_{1i} is the first harmonic field function for the jth deflector, x_i is the rotation angle, and V_x and V_y are the x and y directional deflector voltages.

In the present work the aberration due to misalignment effect in the deflector electrodes is neglected, hence the first term in the right hand side of equation (2-7) was neglected.

2.3. Definitions and Operating Conditions

Some definitions and operating conditions of charged-particle optical systems are given in this section.

Object side: The side of lens or deflector at which the charged particles enter.

Image side: The side of lens or deflector at which the charged particles leave.

The object plane (Z_O): The plane at which the physical object is placed, or a real image is formed from a previous lens or deflector, on the object side.

The image plane (Z_i): The plane at which the real image of the object plane Z_O is formed, on the image side.

Magnification (M): In any optical system the ratio between the transverse dimension of the final image and the corresponding dimension of the original object is called the lateral magnification:

$$M = \frac{image\ height}{object\ height} \quad (2\text{-}10)$$

There are three magnification conditions under which a lens or deflector can operate, namely:

(i) Zero magnification condition: In this operational condition $Z_o = -\infty$ as shown in figure 2-1. As an example, the final probe-forming lens in a scanning electron microscope (SEM) is usually operated under this condition.

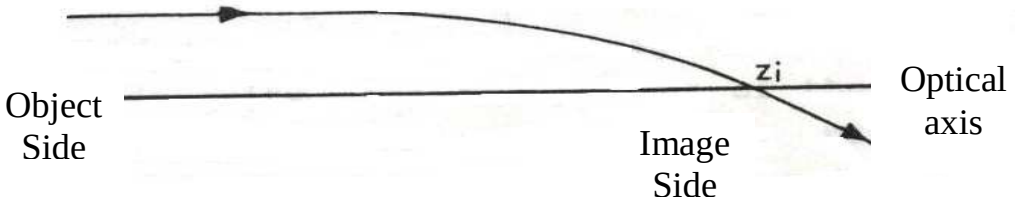

Figure 2-1: Zero magnification condition.

(ii) Infinite magnification condition: In this case $Z_i = +\infty$ as shown in figure 2-2. As an example, the objective lens in a transmission electron microscope (TEM) is usually operated under this condition.

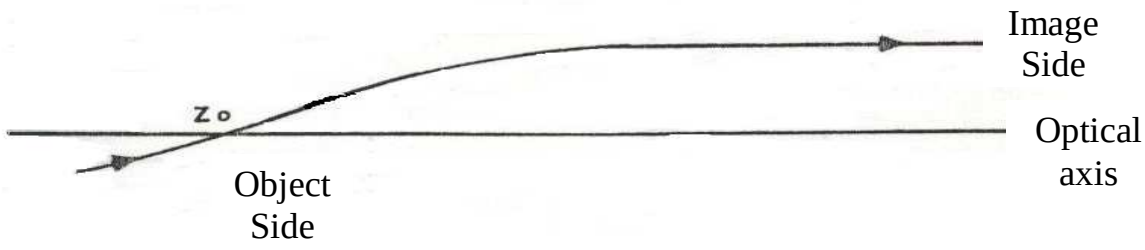

Figure 2-2 : Infinite magnification condition.

(iii) Finite magnification condition: Under this operational condition Z_o and Z_i are at finite distances, as shown in figure 2-3. As an example the electrostatic lens in field-emission gun is usually operated under this condition **(Munro 1975)**.

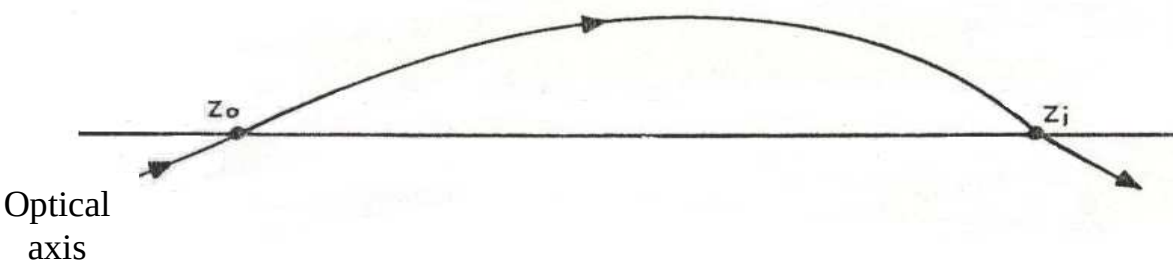

Figure 2-3 : Finite magnification condition.

2.4. Defects of Electron Optical System

The electron paths, which leave points of the object close to the axis at small inclinations with respect to the axis, intersect the image plane in points forming a geometrically similar pattern. This ideal image is known as the Gaussian image, and the plane in which it is formed as the Gaussian image plane. If an electron leaving an object point at finite distance from the axis with a particular direction and velocity intersects the Gaussian image plane at a point displaced from the Gaussian image points, this displacement is defined as *the aberration* **(El-Kareh and El-Kareh 1970)**.

The quality of an electron optical system depends not only upon the wavelength of electrons, but also upon the aberrations from which it may suffer. These aberrations can arise from a number of different reasons. If the accelerating potential fluctuate about his mean value, *chromatic aberration* will mar the image. If the properties of the system are investigated, using a more exact approximation to the refractive index than is employed in the Gaussian approximation, one would find that the geometrical aberrations affect both the quality and the fidelity of the Gaussian image. When the properties of the system are analyzed using the nonrelativistic approximation, the disparities between the relativistic and nonrelativistic can be conveniently regarded as *relativistic aberration*. If, finally, the properties of the system are calculated on the assumption that mechanically, the latter is perfect (i.e. the machining and alignment of all its parts are faultless) the properties of any real system will disagree, to a great or lesser extent, with the calculated values; this is called the *mechanical aberration*. These are the most important types of aberration in electron optical systems, unless there are regions where the electron current density is very high; in such system, the space-charge aberration produced by the interaction between the electron charges may have to be considered **(Hawkes 1967)**.

An example of an optical system with misalignment in the electrodes is shown in figure 2-4. In this figure the lens and deflector electrode shifts to the *x* and *y* direction from the z-axes are approximated using shift function $s_L(z)$ and $s_D(z)$, respectively **(Kurihara 1990)**. Quadrupole lens systems are more sensitive to mechanical defects than round ones **(Baranova and Read 2001)**.

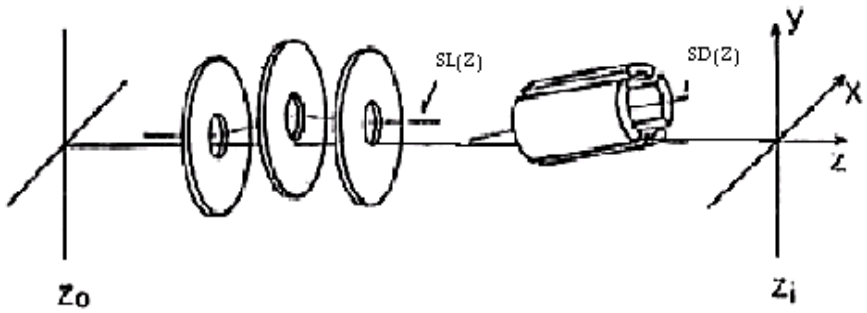

Figure 2-4 : Schematic of the electrostatic system with misalignment. The lens and deflector displacement causes their axis to shift from the optical axis by $s_L(z)$ and $s_D(z)$, respectively **(Kurihara 1990**).

2.5. Aberrations of Axial Symmetrical Optical System

2.5.1 The Spherical Aberration

The spherical aberration is one of the most important geometrical aberrations; this aberrations is sometime, called *aperture defect* and it is one of the principal factors that limit the resolution of the optical system. This defect occurs because the power of the optical system (electrostatic optical system) is greater for off-axis rays than the paraxial rays, i.e. the beams passing within the optical system area at a considerable distance from the axis more (or less) refracted than the paraxial beams so that they intersect closer to (or farther from) the image plane **(Zhigarev 1975)**, as is shown in figure 2-5.

The radius of the spherical aberration disk d_s is given by**(El-Kareh and El-Kareh 1970)** :

$$d_s = C_S \alpha^3 \tag{2-11}$$

where C_s is the spherical aberration coefficient and α is the aperture angle.

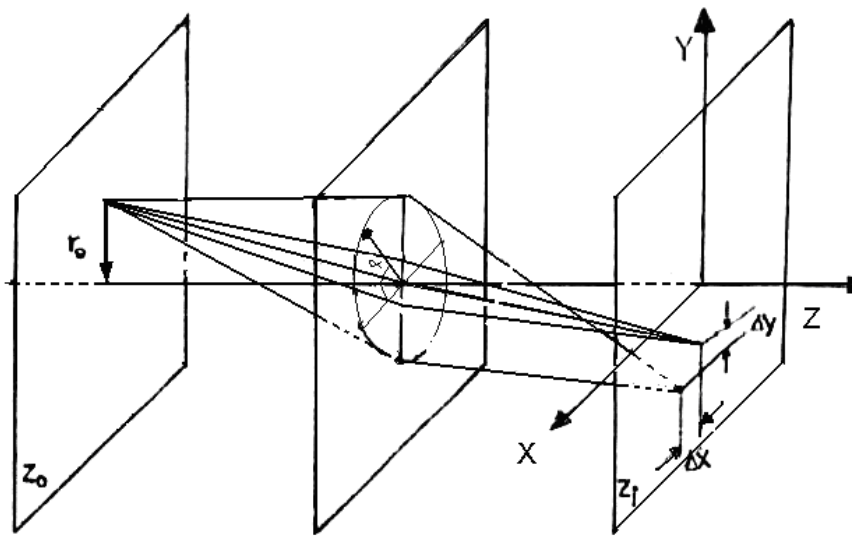

Figure 2-5 : spherical aberration origin **(Ahmad 1993)**.

The spherical aberration coefficient C_{SO} of an axially symmetric electrostatic optical element referred to the object side is given by **(Scheinfein and Galantai 1986, Szilagyi 1987)** :

$$C_{SO}=\frac{U_O^{-1/2}}{16 r_o'^4}\int_{zo}^{zi}\left[\frac{5}{4}\left(\frac{U''}{U}\right)^2+\frac{5}{24}\left(\frac{U'}{U}\right)^2+\frac{14}{3}\left(\frac{U'}{U}\right)^3\frac{r'}{r}-\frac{3}{2}\left(\frac{U'}{U}\right)^2\frac{r'^2}{r^2}\right]\sqrt{U}\, r^4\, dz \qquad (2\text{-}12)$$

where $U=U(z)$ is the axial potential, the primes denote derivatives with respect to z, and $U_O=U(zo)$ is the potential at the object where $z=zo$.

The spherical aberration disk d_s due to misalignment in an axially symmetric electrostatic optical element referred to the object side is given by **(Kurihara 1990**):

$$d_S=\frac{1}{\sqrt{U_o}\, r_o'}\int_{z_o}^{z_i}\sqrt{U}\, r(C_1+C_2-C_3)dz \qquad (2\text{-}13)$$

where

$$C_1=\frac{1}{8\sqrt{U}}(r-U_{SL}{}^2)(U^{-\frac{1}{2}}U''r'+U^{-\frac{1}{2}}U''r''-\frac{1}{2}U^{-\frac{3}{2}}U''r'),$$

$$C_2=\frac{1}{\sqrt{U}}(\frac{1}{4}U^{\frac{1}{2}}U''r'(r-U_{SL})(r'-U'_{SL})+\frac{1}{2}(\frac{1}{2}U^{-\frac{1}{2}}r'^3+3U^{\frac{1}{2}}r'^2r'')),$$

and

$$C_3=(\frac{U''}{4U}(r-U_{SL}))(\frac{U''}{8U}(r-U_{SL})^2+\frac{1}{2}r'^2)+(\frac{U'''}{32U}(r-U_{SL})^3) \qquad (2\text{-}14)$$

for more details see appendix (A).

2.5.2. Chromatic Aberration

The main reason for chromatic aberration is the fact that particles with higher initial energy are less influenced by the imaging field than lower-energy particles. Therefore, if all particles leave the object point with the same slope, the high-

energy particles will form an image at a greater distance from the object than the particles of low energy and the image will be blurred like in case of spherical aberration. There are several reasons for the energy spread of the particles; first of all, no source can produce a monochromatic beam of particles. The initial velocities of different particles of the beam are all different, which corresponds to different value of U_o in the axial potential distribution. This effect is especially harmful for low-energy beams where the magnitude of the energy spread may be comparable with his average beam energy **(Szilagyi 1988)**.

Chromatic aberration can be simplified with the aid of the following example. If a parallel beam is incident on a lens, leaves it with momentum "p" then for perfect lens it will be focused at a focal point z_i on th z-axis. Particles with momentum $(p+\Delta p)$ on the other hand are focused at $z=z_i + (\Delta f/\Delta p)\Delta p$ as shown in figure 2-6 where f is the focal length of the lens. If the angle of convergence of the rays is α, then the radius of least confusion d_c (radius of chromatic aberration disk), is given by, (**Lawson 1977**).

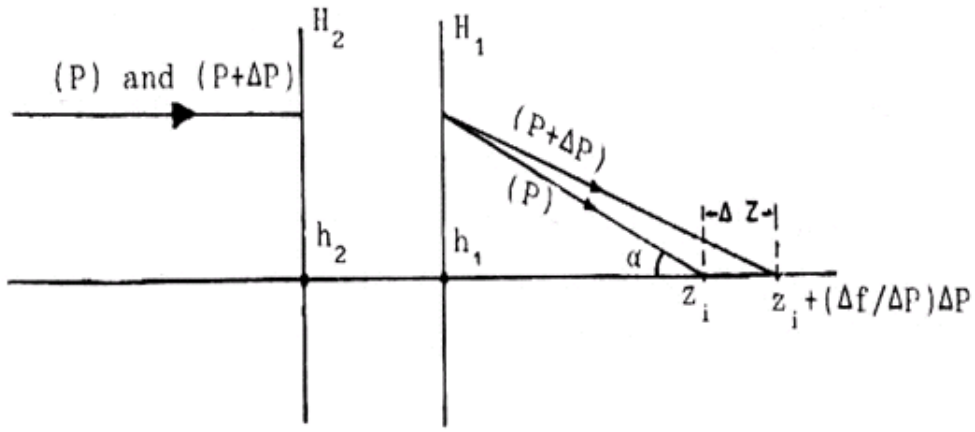

Figure 2-6 : chromatic aberration origin **(Ahmad 1993)**.

$$d_C = \alpha\left[\frac{\Delta f}{\Delta p}\right]\Delta p = \alpha f\left[\frac{p}{f}\right]\frac{\Delta p}{p} \qquad (2\text{-}15)$$

The coefficient of chromatic aberration Cc is :

$$Cc/f = (1/2)(p/f)(\Delta f/\Delta p) \qquad (2\text{-}16)$$

from equations (2-15) and (2-16) it follows for the non relativistic case that:

$$d_C = Cc\alpha\Delta E/E \qquad (2\text{-}17)$$

where E is the potential energy through which the charged-particles have been accelerated to reach the momentum p, and ΔE refers to half the total energy spread in the beam **(Lawson 1977)**.

The total radius of the aberration disk d_t is :

$$d_t = \sqrt{d_s{}^2 + d_c{}^2} \qquad (2\text{-}18)$$

The chromatic aberration coefficient Cc of electrostatic optical element, with axial symmetric field condition, is given by **(Scheinfein and Galantai 1986, Szilagyi 1987, Kiss 1988)**:

$$C_{CO} = \frac{\sqrt{U_O}}{r_O'^2}\int_{z\circ}^{zi}\left[\frac{1}{2}\left(\frac{U'}{U}\right)r' + \frac{1}{4}\left(\frac{U''}{U}\right)r\right]\frac{r}{\sqrt{U}}\,dz \qquad (2\text{-}19)$$

where the parameters in this equation are the same as those used in equation (2-12).

The chromatic aberration disk d_C due to misalignment in an axially symmetric electrostatic optical element referred to the object side is given by **(Kurihara 1990**):

$$d_c = -\frac{1}{\sqrt{U_o}\, r_o'} \int_{zo}^{zi} \sqrt{U}\, r P_c\, dz \qquad (2\text{-}20)$$

where

$$p_c = \frac{\Delta E}{E}\left(\frac{U'}{2U} r' + \frac{U''}{4U}(r - U_{SL}) + \frac{VF_1}{2U}\right) \qquad (2\text{-}21)$$

In the present work the effect of misalignment in deflector was neglected, hence the last term in right hind side of equation (2-21) neglected.

2.6. Immersion Lens

In the optical sense the two-cylinder lens is properly of the immersion type, since object and image space differ in potential and hence in refractive index. It is convenient in electron optics, howefer, to reserve the title to those lenses in which the object is deeply immersion in the field, so that the refractive index varies rapidly in its neighborhood.

An immersion lens, as almost every other electron lens, consist of two or more thin lenses of different properties. On the low-potential side, the lens is of a converging character whereas on the high-potential side it is diverging. Its overall action, however, is converging **(Paszkowski 1968).** Immersion lenses accelerate or retard the charged particles while the beam is focused and may consist of as few as two electrodes **(Baranova and Yavor 1984)**.

2.7. Einzel (Unipotential) Lens

The most commonly used einzel (unipotential) lenses have three electrodes. The distinctive feature of einzel lenses is that they have the same constant potential U_1 at both the object and the image side, the central electrode is at a different potential U_2, therefor, they are used when only focusing is required but the beam energy must be retained.

Einzel (unipotential) lenses are symmetrical with respect to the center of the lens for both of its foci. Hence, they are frequently called symmetrical lenses **(Paszkowski 1968**). The symmetrical lens is usually possible, of course, to destroy the symmetry by applying different voltages to the two outer electrodes and still have a practicable lens. The focusing action of the system remains essentially the same in the symmetrical case, but it is not in general used owing to the obvious advantages of the latter **(Cosslett 1950)**.

2.8.Computer Programs

2.8.1. Computer Programs for Computing the Beam Trajectory and the Optical Properties

A computer program written by **Munro (1975)** and then modified by **Ahmad (1993)** has been used to determine the trajectory of the charged particles using the Runge-Kutta method, with initial conditions depending on the magnification of the lens. Optical properties such as the focal length and aberration are calculated by integrating the paraxial-ray equation. The integration was performed using Simpson's rule. A Personal Computer has been used for executing the above work.

2.8.2. Electrode Shape Progam

With the aid of the computer program written by **Ahmad (1993)** in Fortran 77 the profile of the electrodes producing a certain electrostatic lens can be determined by the following equation of an equipotential surface **(Szep and Szilagyi 1987)**:

$$R = 2((U(z) - u(r,z))/U''(z))^{1/2} \qquad (2\text{-}24)$$

where u(r,z) is the off-axis potential, U(0,z) is the axial potential function whose number of its inflection points are counted. The radial displacement r approaches infinity at each inflection point where U''(0,z)=0. the number of electrodes is greater than the number of inflection points by one. If the value of the second derivative is negative between two inflection points or between the start/end point and the nearest inflection point, then the electrode potential which is slightly higher than the maximum value of the axial potential in this interval is chosen. If the second derivative is positive, the chosen electrode potential must be lower than the minimum value of the axial potential **(Szilagyi 1988)**.

3. RESULTS AND DISCUSSION

3.1. Immersion Lens Without Misalignment Effect

The potential distribution of an immersion lens has been suggested to represent an immersion electrostatic lens and it has the following form to fit for the curve shown in figure 1-1a which represent the potential distribution along the optical axis of an immersion lens:

$$U(z) = a + b\tanh(z+1) \qquad (3\text{-}1)$$

where a and b are constant effecting the value of the voltage ratio of the two electrodes that form an immersion lens. The constant a and b has the unit of volt to match the unit of U(z).

The potential distribution of the immersion lens is shown in figure 3-1 with the corresponding first and second derivatives along the optical axis z based on the proposed expression given in equation (3-1).

Figure 3-1 shows the case of an accelerating potential (accelerating lens) since U2/U1 is greater than unity (= 4), with constant a=6 and b=3.6 hear. The second derivative of U(z) has one inflection point this result suggests that the lens has two electrodes since the number of electrode is greater than the number of inflection point in U"(z) by one as mention in chapter two. The electrodes profile shown in figure 3-2a. It is obvious that the two electrodes are different in size but identical in shape and have a shape of a letter L.

Figure 3-2a also shows the values of the inner and outer radii of the two electrodes in term of the lens length L which is equal to 20mm, R_{in}=0.05L and R_{out} =0.38L respectively. The air gap separating the two electrodes is 0.04L and this gap is enough to avoid the electrical breakdown between the two electrodes.

Under usual condition of vacuum the electrodes must be separated from each other so that the maximum field strength dose not exceed 15 kV/mm **(Szilagyi 1988)**. Rotation of the electrodes profile about the optical axis produces a 3-D diagram is shown in figure 3-2b.

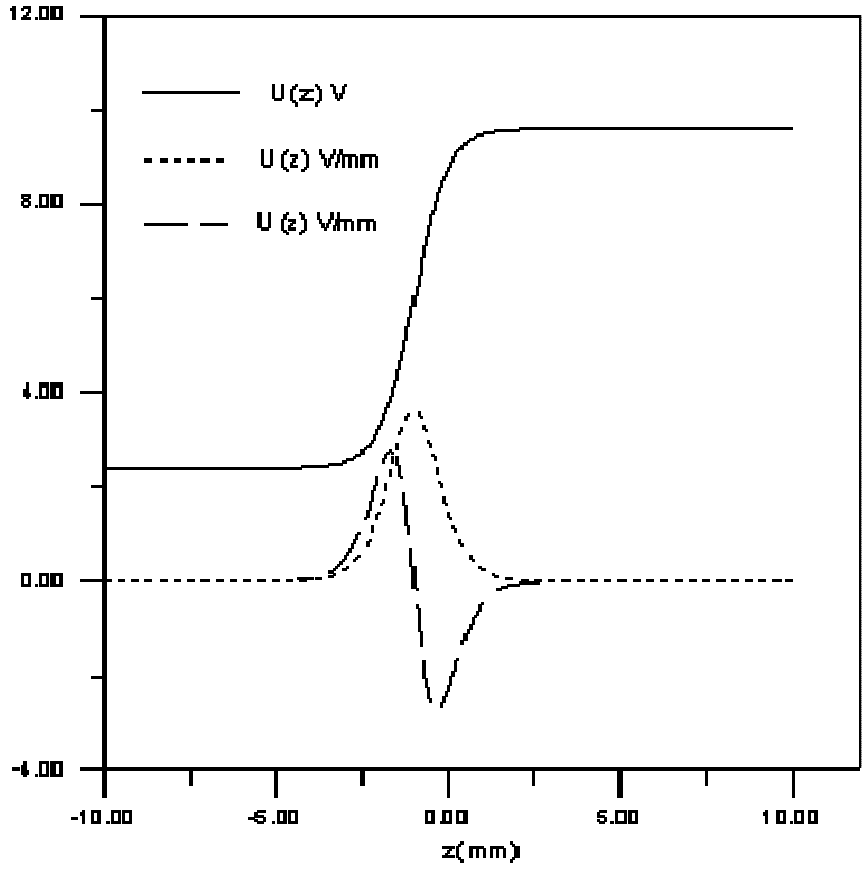

Figure 3-1: The axial potential distribution U(z) and its first and second derivatives U′(z) and U″(z) respectively of the immersion lens.

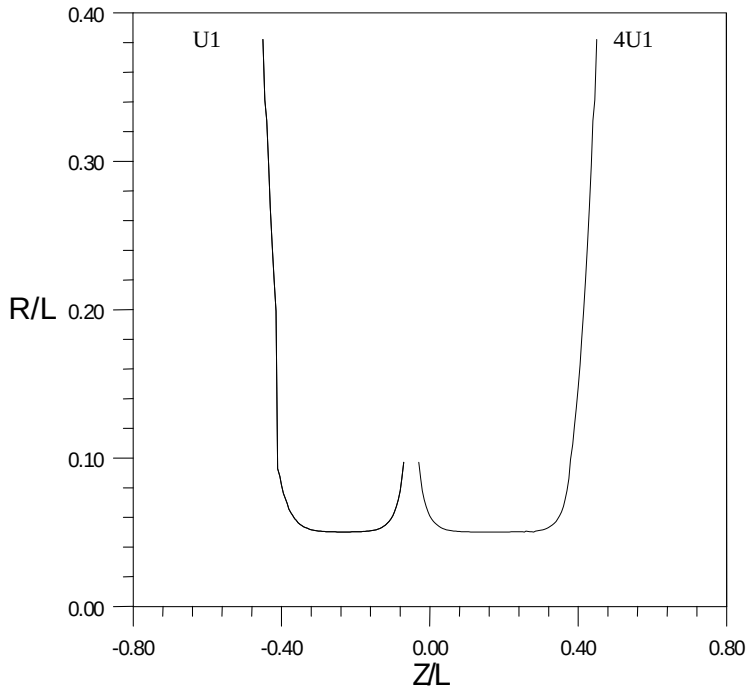

(a)

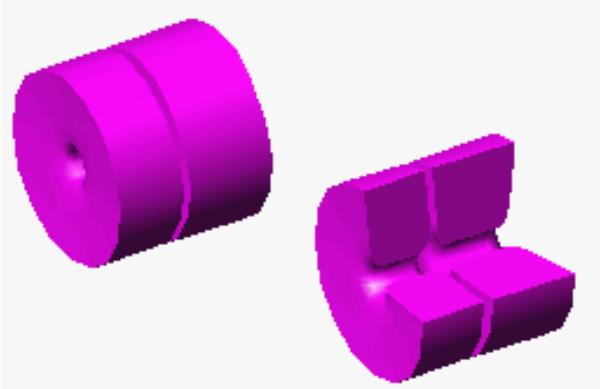

(b)

Figure 3-2 : (a) The profile of the two-electrode immersion lens. (b) A three-dimensional diagram of the two-electrode immersion lens.

The electrode voltage ratio U2/U1 of the immersion lens whose axial potential distribution is shown in figure 3-1 can be varied if the constant b given in equation (2-22) is changed. The relation between the constant b and the electrode voltage ratio U2/U1 is shown in figure 3-3. It can be seen that U2/U1 increases with increasing the constant b. However, at values of the constant b>4.68, the variation of the voltage ratio becomes more significant.

The beam trajectories for the two electrode immersion lens under zero and infinite magnification condition are shown in figures 3-4a and 3-4b respectively.

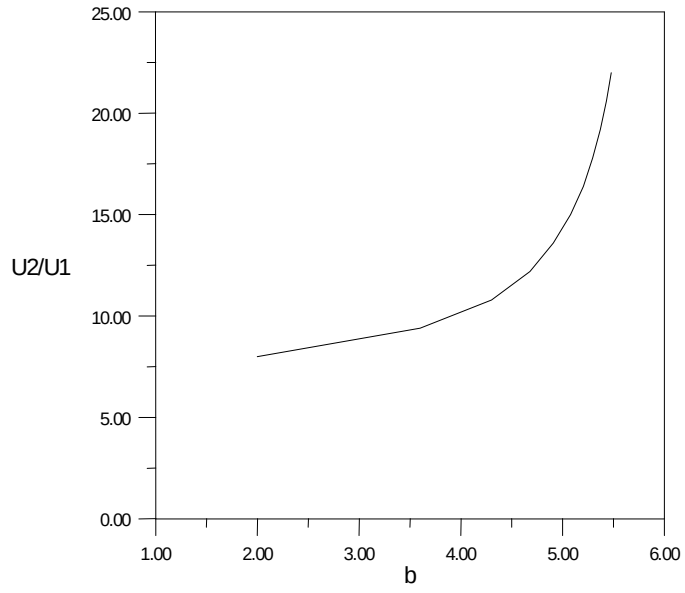

Figure 3-3 : Variation of the electrodes voltage ratio with the constant b for two electrode immersion lens.

The focal length of the immersion lens has been normalized in terms of the length of lens field L. The relative image-and object-side focal lengths of the immersion lens depend on the electrode voltage ratio U2/U1 as shows in figure 3-5a and 3-5b respectively. It is clear that the relative image-and object-side focal lengths decreases with increasing voltage ratio U2/U1, i.e. the lens become stronger or its refractive power become longer.

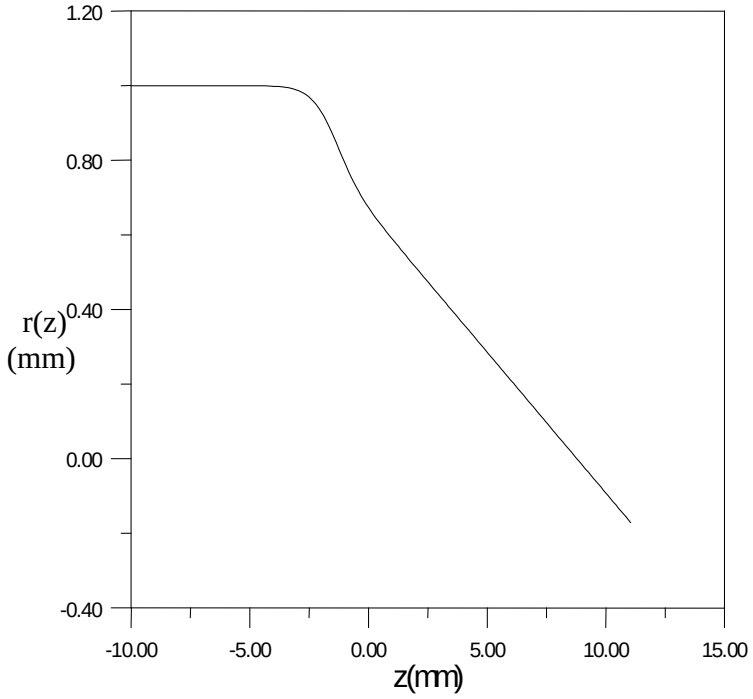

(a)

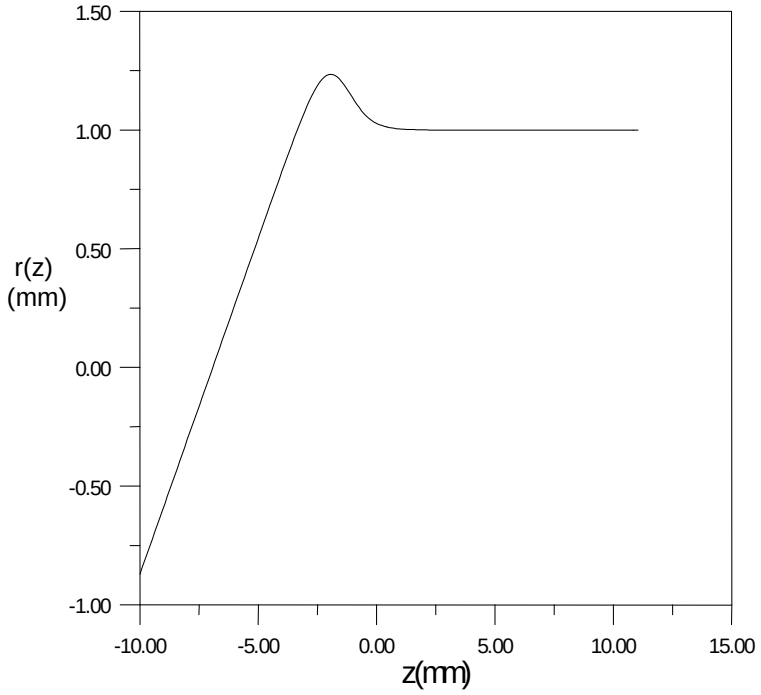

(b)

Figure 3-4 : The trajectory along the optical axis of the two electrode immersion lens under (a) Zero magnification condition and (b) Infinite magnification condition.

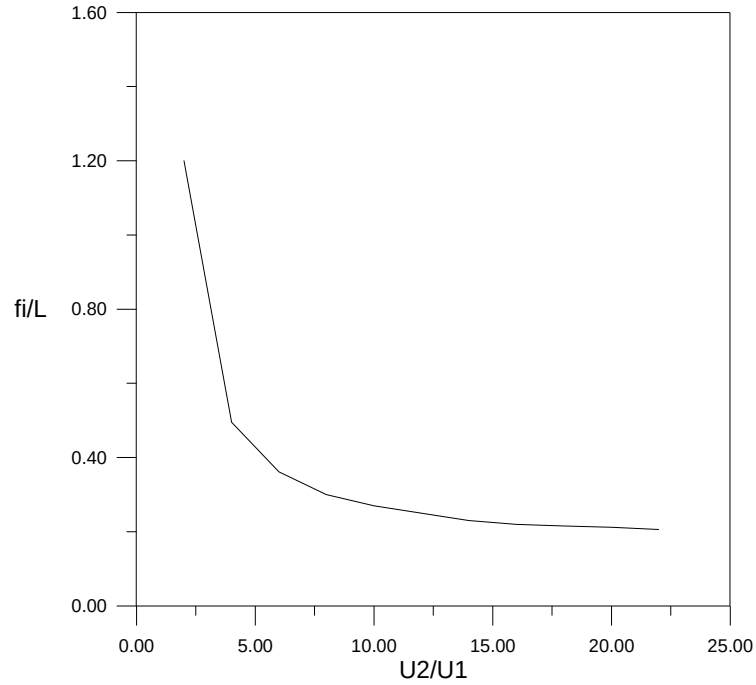

(a)

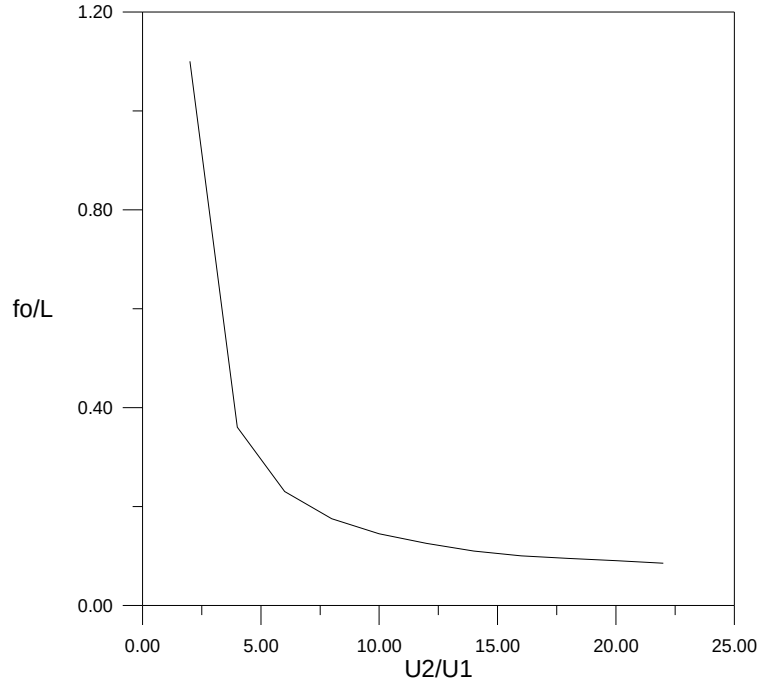

(b)

Figure 3-5 : The relative focal length of the two electrode immersion lens as a function of voltage ratio Under (a) Zero magnification condition and (b) Infinite magnification condition.

The spherical and chromatic aberrations have been given considerable attention in the present work since they are the most important parameters in electron optical systems.

Figures 3-6 and 3-7 represent the behavior of spherical, chromatic and total aberration disks d_s, d_c and d_t respectively for the immersion lens on a logarithmic scale as functions of the voltage ratio U2/U1. Taking into account the values of the half acceptance angle α =5mrad and the energy spread $\Delta E/E=1*10^{-4}$ which are usually taken in to consideration in the literature **(Scheinfein and Galantai 1986; Szilagyi 1988)**.

Figure 3-6 shows the behavior of spherical, chromatic and total aberration disks d_s, d_c and d_t respectively under zero magnification condition. It is obvious that the spherical, chromatic and total aberration disks decreases with increasing voltage ratio U2/U1. At values of U2/U1<6, the spherical aberration disk is the dominant factor while at U2/U1>8 the chromatic aberration disk becomes the dominant factor. The minimum values of spherical, chromatic and total aberration disk are 1.67µm at U2/U1=22, 17.229µm at U2/U1=16 and 17.301µm at U2/U1=18 respectively.

Figure 3-7 shows the behavior of spherical, chromatic and total aberration disks d_s, d_c and d_t respectively under infinite magnification condition. It is seen that the spherical, chromatic and total aberration disks decreases with increasing voltage ratio U2/U1, i.e. the same behavior are in the zero magnification condition. The total aberration disk d_t is very close to the spherical aberration disk at U2/U1<6; but when U2/U1 exceeds 6 the chromatic aberration disk becomes dominant. The minimum values of spherical, chromatic and total aberration disks are 0.256µm, 4.091µm and 4.098µm respectively at U2/U1=22.

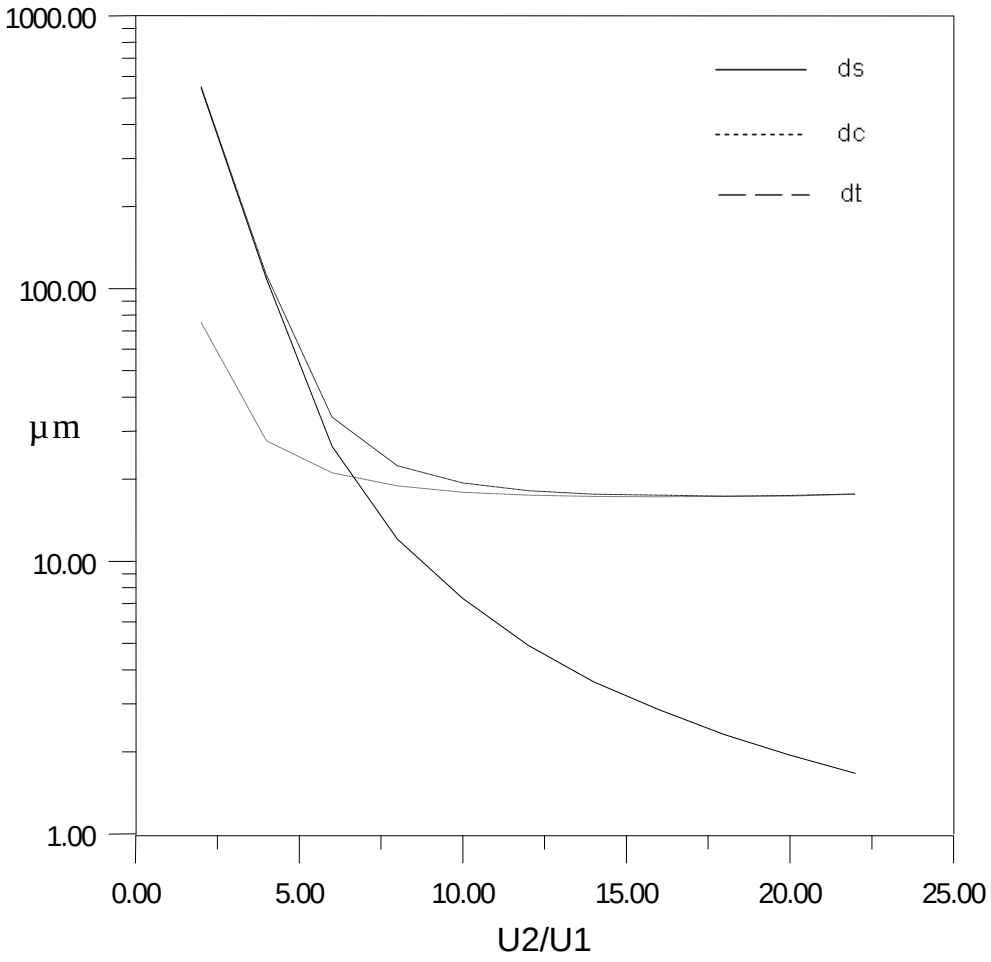

Figure 3-6 : The spherical, chromatic and total aberration disks of a two-electrode immersion lens as a functions of voltage ratio U2/U1 operated under zero magnification condition.

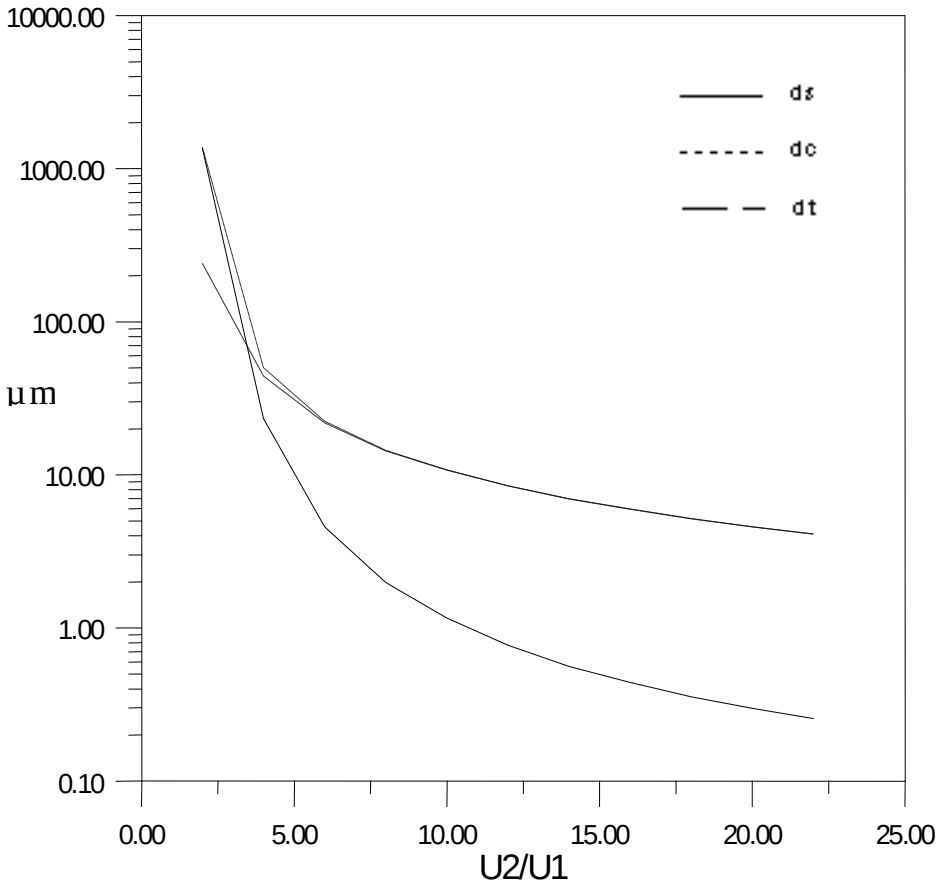

Figure 3-7: The spherical, chromatic and total aberration disks of a two-electrode immersion lens as a functions of voltage ratio U2/U1 operated under infinite magnification condition.

3.2. Immersion Lens With Misalignment Effect

The electrostatic lens which including the misalignment effect approximated by introducing a shift function $U_{SL}(z)$ given in equation (2-5) that expresses the electrode shift from the optical axis. The behavior of shift function $U_{SL}(z)$ is shown in figure 3-8.

Figure 3-9 shows the behavior of the two electrodes immersion lens which they shift from the optical axis z due to misalignment effect.

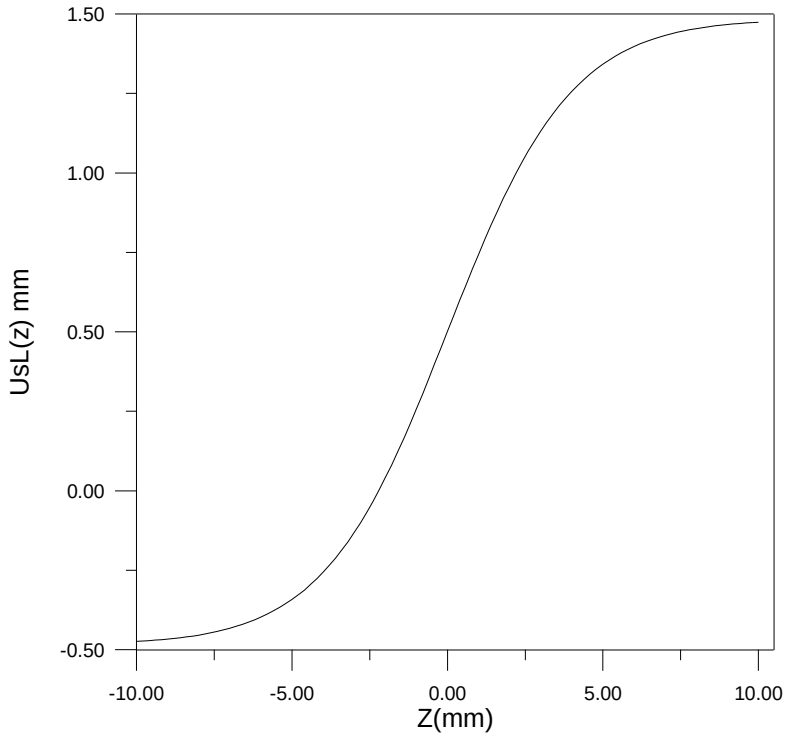

Figure 3-8: The behavior of the shift function that expresses the electrode shift from the optical axis z.

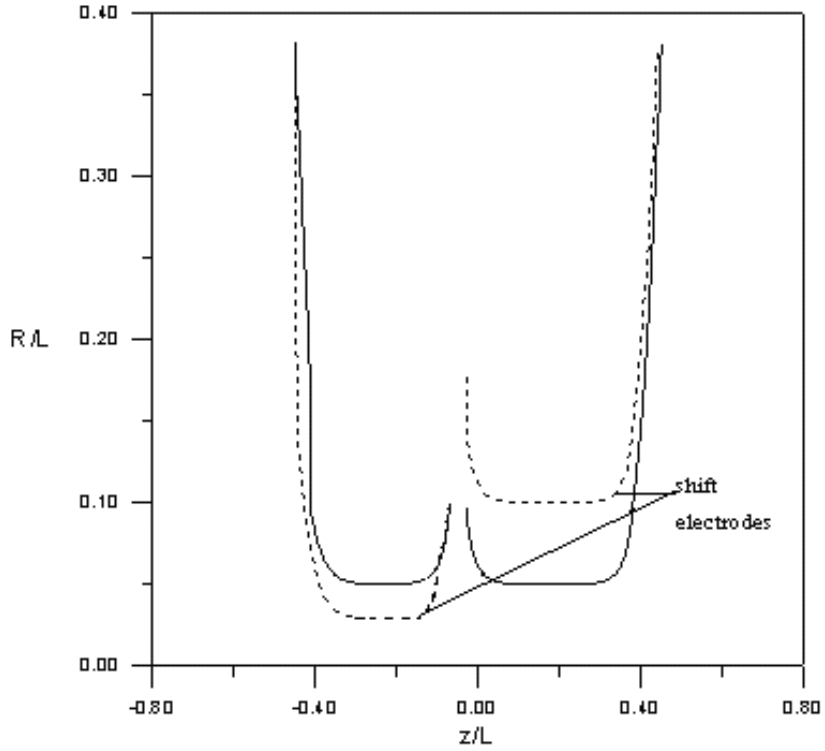

Figure 3-9 : The profile of the two electrode immersion lens with and without misalignment effect.

The beam trajectories for the immersion lens which including misalignment effect under zero and infinite magnification conditions are shown in figure 3-10a and 3-10b respectively.

The relative image-and object-side focal lengths of the immersion lens which including misalignment effect depends on the electrode voltage ratio U2/U1 as shown in figure 3-11a and 3-11b, respectively. It is clear that the relative image- and object-side focal lengths decreases with increasing voltage ratio U2/U1, i.e. the lens become stronger or its refractive power become longer.

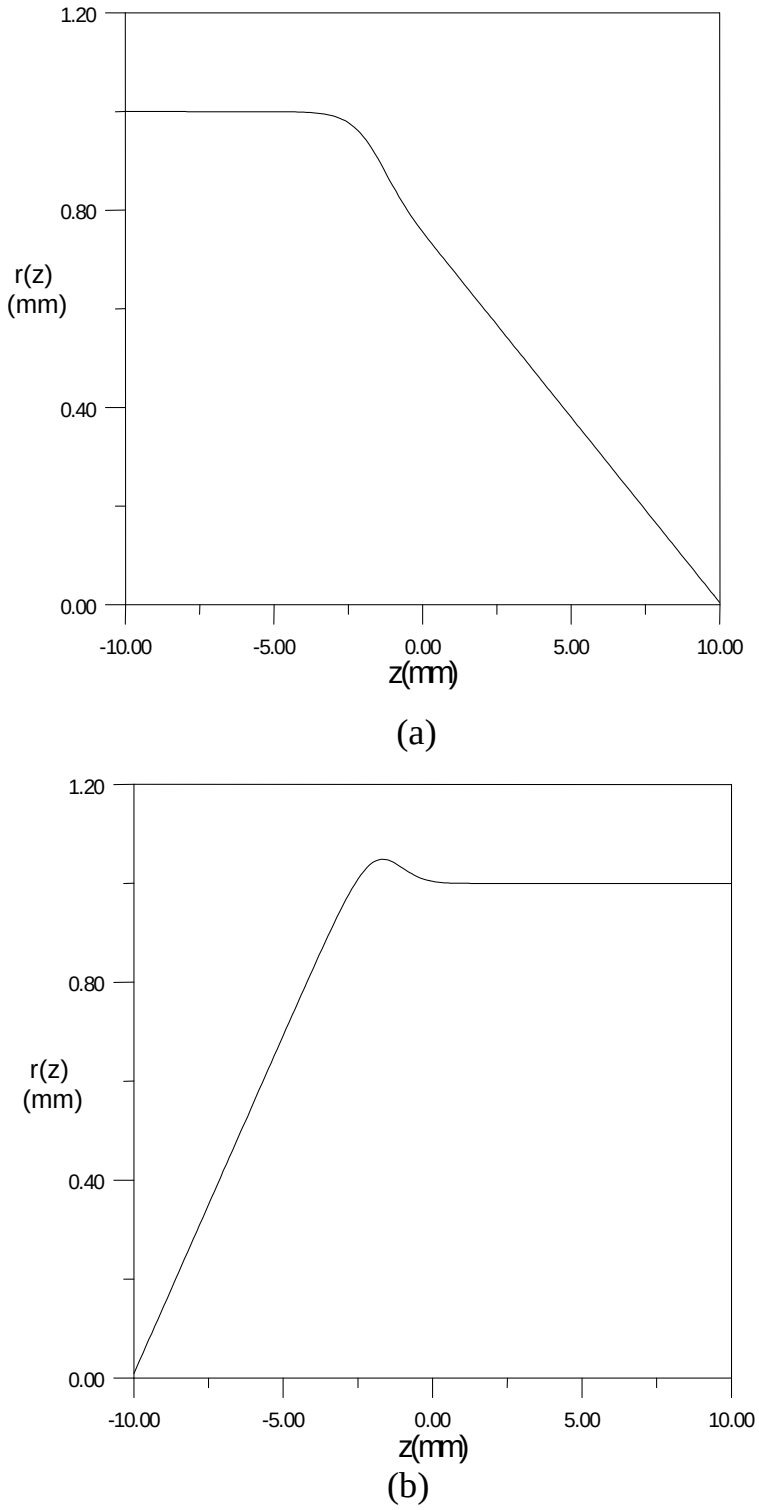

Figure 3-10: The trajectory along the optical axis of the immersion lens which including misalignment effect under (a) Zero magnification condition and (b) Infinite magnification condition.

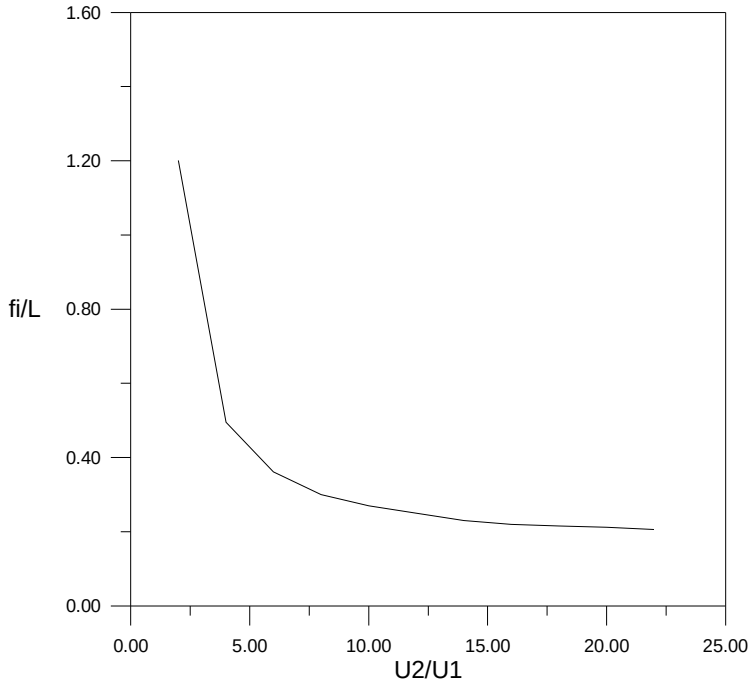

(a)

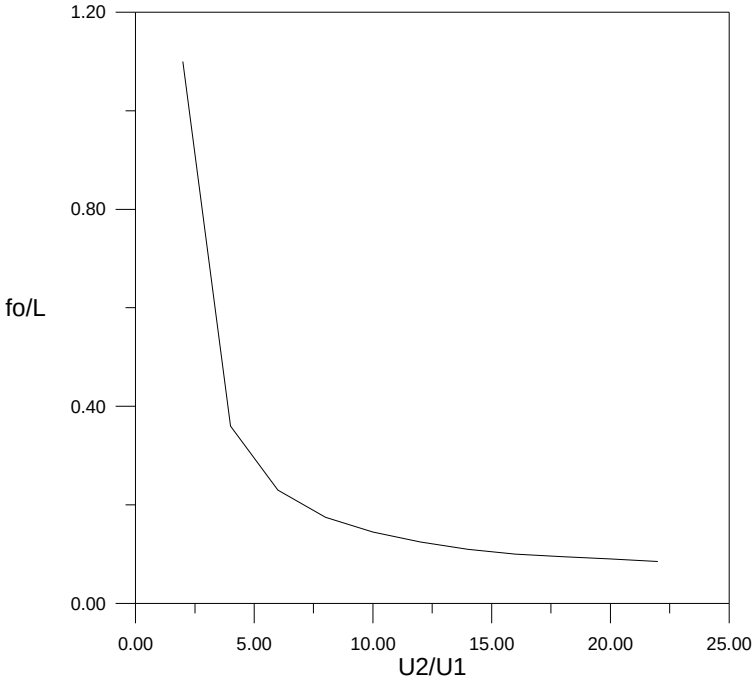

(b)

Figure 3-11: The relative focal length of the two electrode immersion lens which including misalignment effect as a function of voltage ratio under (a) Zero magnification condition (b) Infinite magnification condition.

The relation between spherical, chromatic and total aberration disks d_s, d_c and d_t respectively for the immersion lens which including misalignment effect on a logarithmic scale with voltage ratio U2/U1 is shown in figures 3-12 and 3-13.

Figure 3-12 shows the behavior of spherical, chromatic and total aberration disks d_s, d_c and d_t respectively under zero magnification condition. The spherical aberration disk d_s decreases and chromatic aberration disk d_c increases with increasing voltage ratio U2/U1. The spherical and chromatic aberration disk become equal and have a value of 4.434µm at U2/U1=10.3. At values U2/U1<8, the spherical aberration disk is the dominant factor while at U2/U1>12 the chromatic aberration disk becomes dominant. The minimum values of spherical, chromatic and total aberration disks are as follows:

d_s = 0.25µm at U2/U1= 22.

d_c= 0.68µm at U2/U1 = 2.

d_t =4.667µm at U2/U1 = 22.

Figure 3-13 shows the variation of spherical, chromatic and total aberration disks d_s, d_c and d_t respectively with U2/U1 under infinite magnification condition. It is clear that the spherical and chromatic aberration disks are increases with increasing voltage ratio U2/U1. The curves d_s and d_t coincide indicating that the value of spherical aberration disk d_s is always dominant. The minimum values of spherical, chromatic and total aberration disks are 51.91µm, 0.468µm and 51.912µm respectively at U2/U1=2.

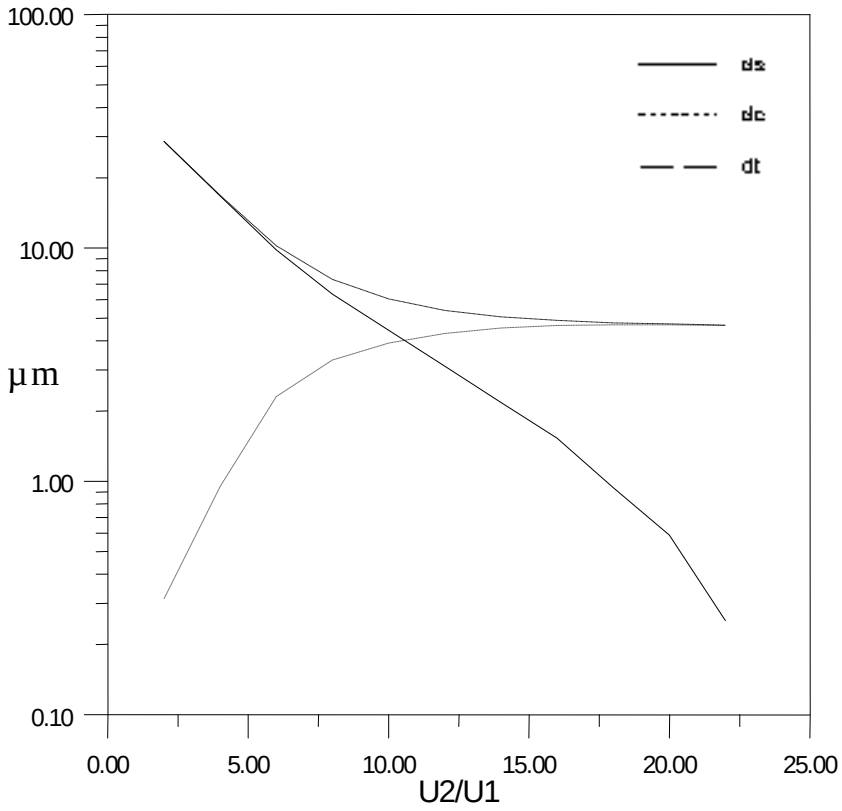

Figure 3-12: The spherical, chromatic and total aberration disks of a two-electrode immersion lens which including misalignment effect as a functions of voltage ratio U2/U1 operated under zero magnification condition.

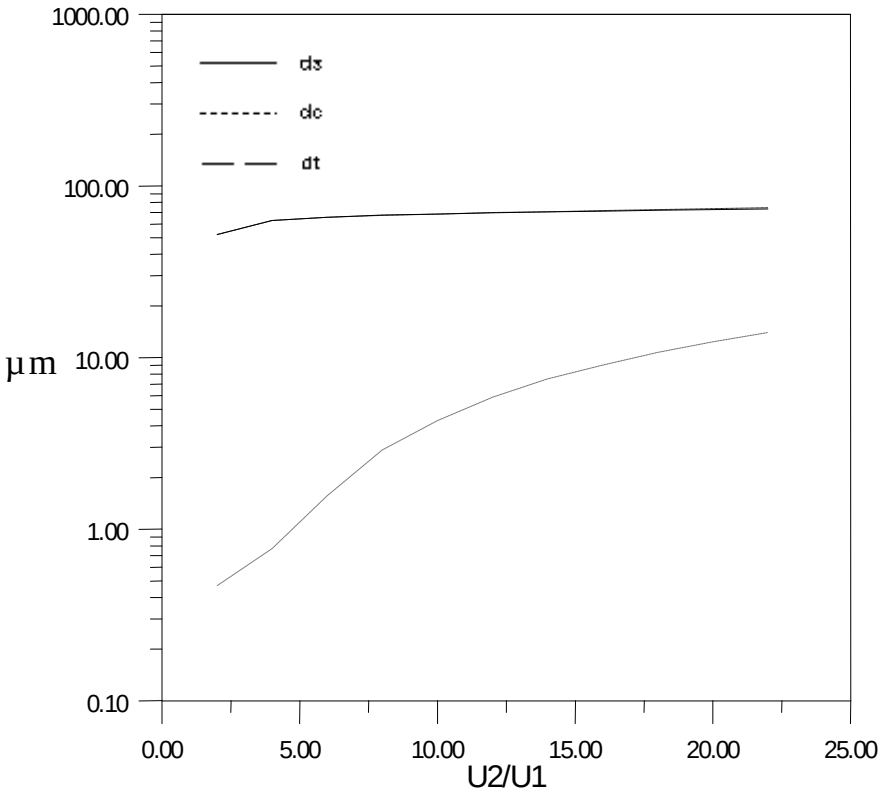

Figure 3-13: The spherical, chromatic and total aberration disks of a two-electrode immersion lens which including misalignment effect as a function of voltage ratio U2/U1 operated under infinite magnification condition.

3.3. Einzel Lens Without Misalignment Effect

It is aimed in the present work to find a more simple analytic expression that would describe the axial potential distribution of einzel lenses with electron optically acceptable aberrations. The following expression is suggested to fit for the curve shown in figure 1-1f which represent the potential distribution along the optical axis of an einzel lens:

$$U(z) = a + be^{\left(-cz^2\right)} \qquad (3\text{-}2)$$

where a, b and c are constant effecting the value of the ratio of voltage applied on the central and outer electrodes. The constant a and b has the unit of volt and c has the unit of mm^{-2} to match the unit of U(z).

The axial field distribution given in equation (3-2) for an einzel lens is shown in figure 3-14 with its first and second derivatives along the optical axis z. This field has been used for determining the trajectory and the aberration of the lens.

The potential distribution U(z) is constant at the boundaries, hence its first derivative U′(z) is zero. This indicates that there is no electric field outside the lens i.e. there is a field-free region away from the lens terminals where the trajectory of the charged particles beam is a straight line due to the absence of any force acting on it. The lens has three electrodes since the second derivative of the potential U″(z) has two inflection points.

The profile of the three electrodes forming an electrostatic einzel lens is shown in figure 3-15a. The lens is symmetrical about its center in addition to the rotational symmetry.

A three-dimensional (3-D) diagram is shown in figure 3-15b for the three electrodes forming an electrostatic lens. The central electrode is in the form of disk

with central hole of a radius equivalent to 0.0012L to allow passing for the accelerated charged particles beam and with outer radius equal to 0.093. The two outer electrodes are geometrically identical in shape similar to that of central electrode, and both have an inner hole of a radius equal to 0.04L and outer radius equal to 0.2L. Two equal gaps of 0.02L are found to separate each of the outer electrodes from central one.

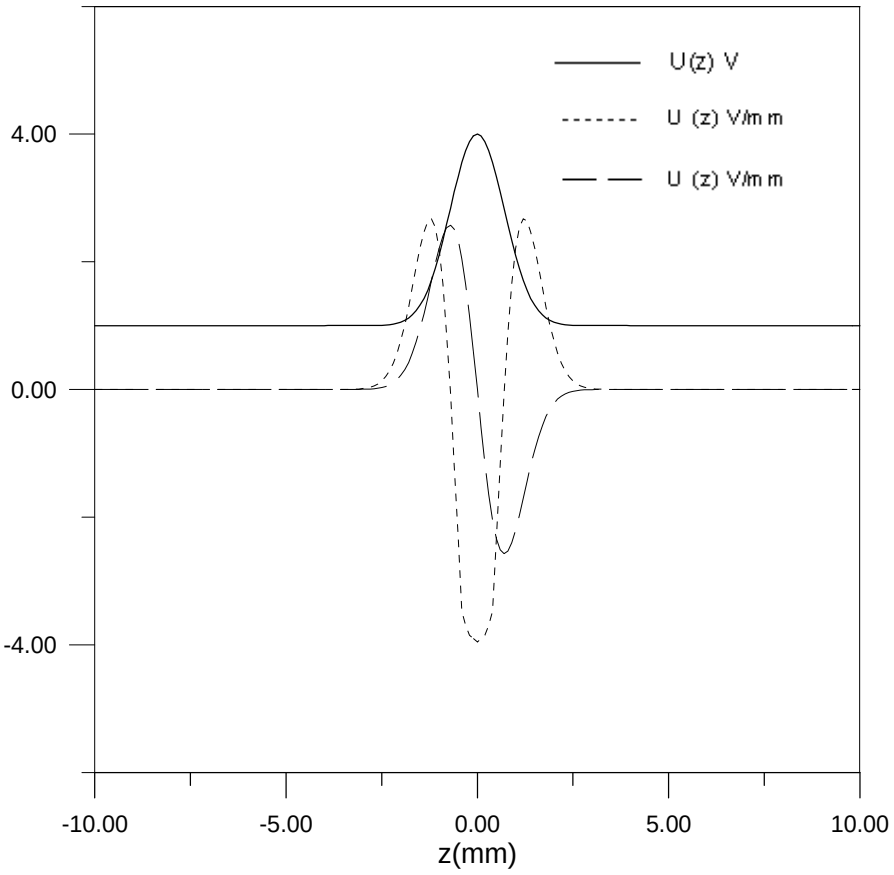

Figure 3-14 : The axial potential distribution U(z) and its first and second derivatives U′(z) and U″(z)respectively of an einzel lens.

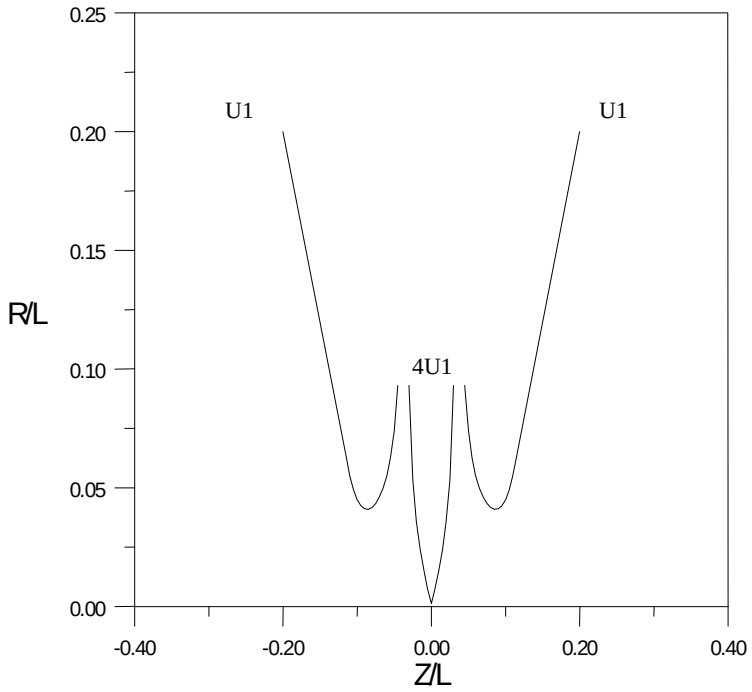

(a)

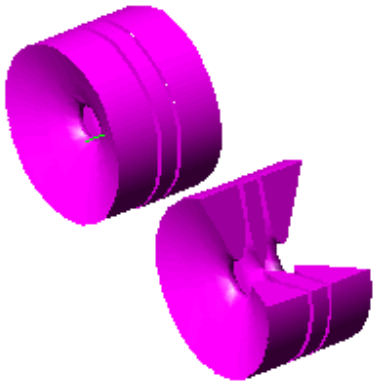

(b)

Figure 3-15 : (a) The profile of the three-electrode einzel lens. (b) A three-dimensional diagram of the three-electrode einzel lens.

The effect of the electrode voltage ratio is one of the most important parameter on the optical properties of various electrostatic lenses. If the constant b given in equation (2-23) is changed the electrode voltage ratio U2/U1 of an einzel lens whose axial potential distribution is shown in figure 3-14 is changed. The dependence of the electrodes voltage ratio on the constant b is shown in figure 3-16. It is clear that the voltage ratio is a linear function of the constant b, the voltage ratio increases with increasing the constant b.

Figures 3-17a and 3-17b show the beam trajectories under zero and infinite magnification condition respectively.

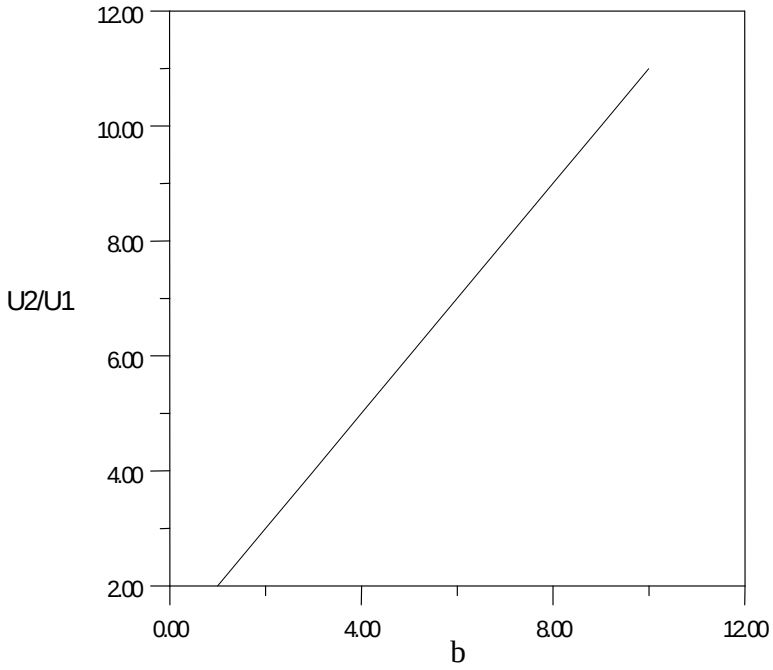

Figure 3-16 : Variation of the electrodes voltage ratio with the constant b for three-electrode einzel lens.

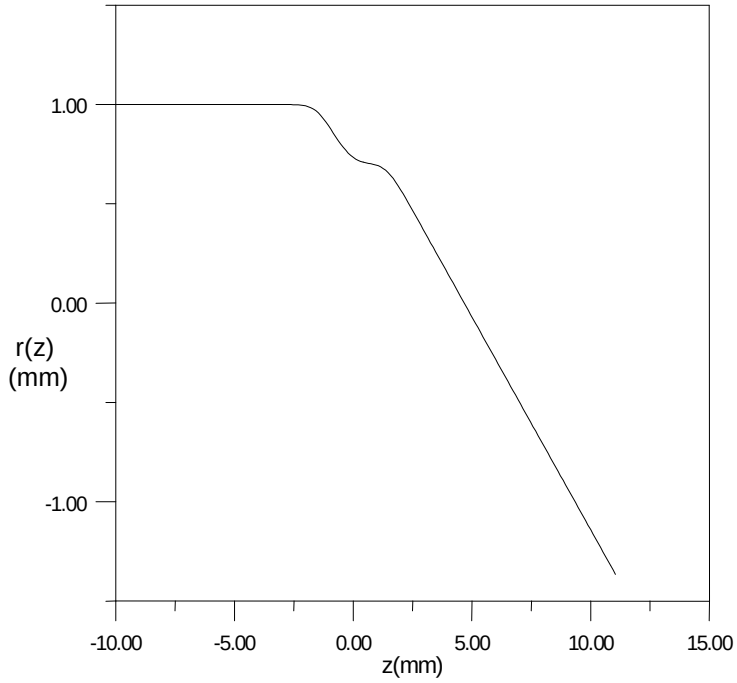

(a)

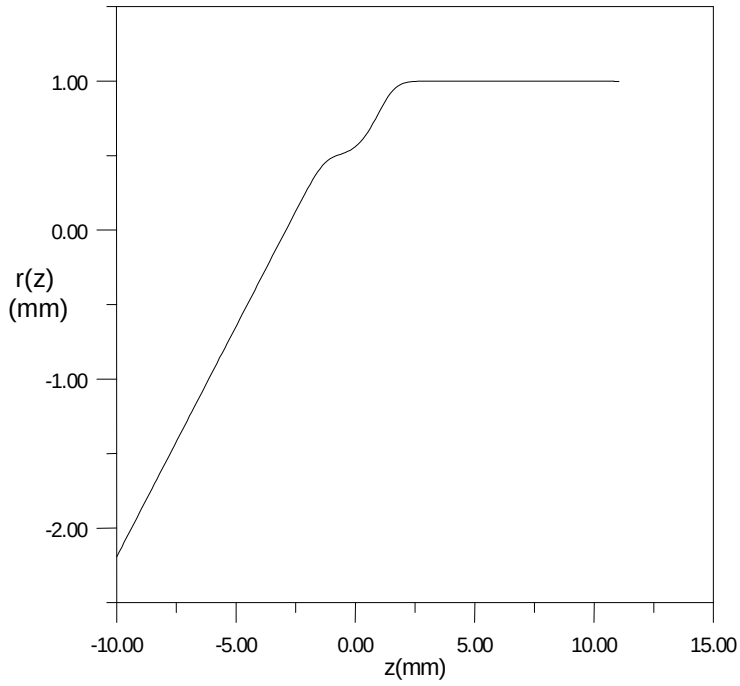

(b)

Figure 3-17 : The trajectory along the optical axis of the einzel lens under (a) Zero magnification condition and (b) Infinite magnification condition.

The focal length of the einzel lens has been normalized in terms of the length of lens field L, thus the focal length is a dimensionless quantity. The relative image- and object-side focal lengths of the einzel lens depend on the electrode voltage ratio U2/U1 as shown in figure 3-18a and 3-18b respectively. It is clear that the relative image-and object-side focal lengths decreases with increasing voltage ratio U2/U1, i.e. the lens become stronger or its refractive power become longer.

Figures 3-19 and 3-20 represent the behavior of spherical, chromatic and total aberration disks d_s, d_c and d_t respectively for an einzel lens on a logarithmic scale as functions of the voltage ratio U2/U1.

Figure 3-19 shows the behavior of spherical, chromatic and total aberration disks d_s, d_c and d_t respectively under zero magnification condition. It is obvious that the spherical, chromatic and total aberration disks decreases with increasing voltage ratio U2/U1. At low values of voltage ratio U2/U1, the decrease of both spherical and chromatic aberration disks is rapid. At values of U2/U1>5, the variations are less sensitive. The total aberration disk d_t is close to the spherical aberration disk d_s at U2/U1<3; but when the electrode voltage ratio U2/U1 exceeds 3 the chromatic aberration disk d_c becomes dominant, approaching the value of d_t. The minimum values of spherical, chromatic and total aberration disks are 0.376µm, 6.557µm and 6.567µm respectively at U2/U1≒11.

Figure 3-20 shows the behavior of spherical, chromatic and total aberration disks d_s, d_c and d_t respectively under infinite magnification condition. It is clear that the spherical and chromatic aberration disks have the same behavior. At low value of U2/U1, the spherical and chromatic aberration disks d_s and d_c respectively decreases. At U2/U1 exceeds 7, the variations of d_s and d_c increases. At values U2/U1<4 the spherical aberration disk is the dominant factor. The minimum values of spherical, chromatic and total aberration disks are 0.637µm, 0.815µm and 1.034µm respectively at U2/U1=7.

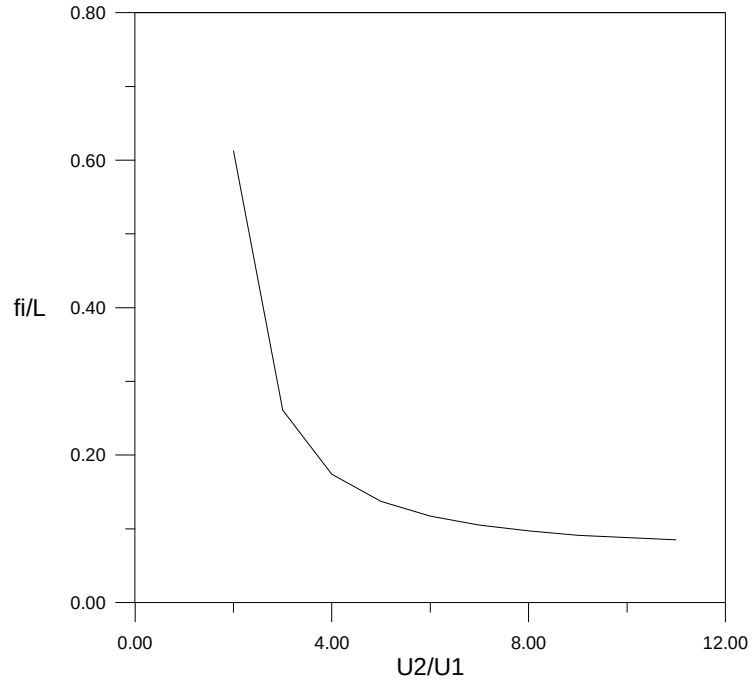

(a)

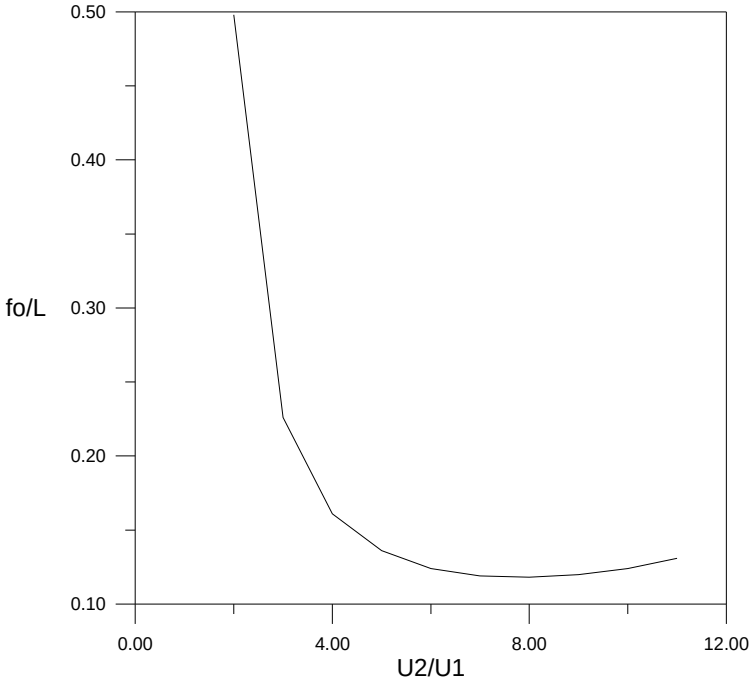

(b)

Figure 3-18 : The relative focal length of the three electrode einzel lens as a function of voltage ratio under (a) Zero magnification condition (b) Infinite magnification condition.

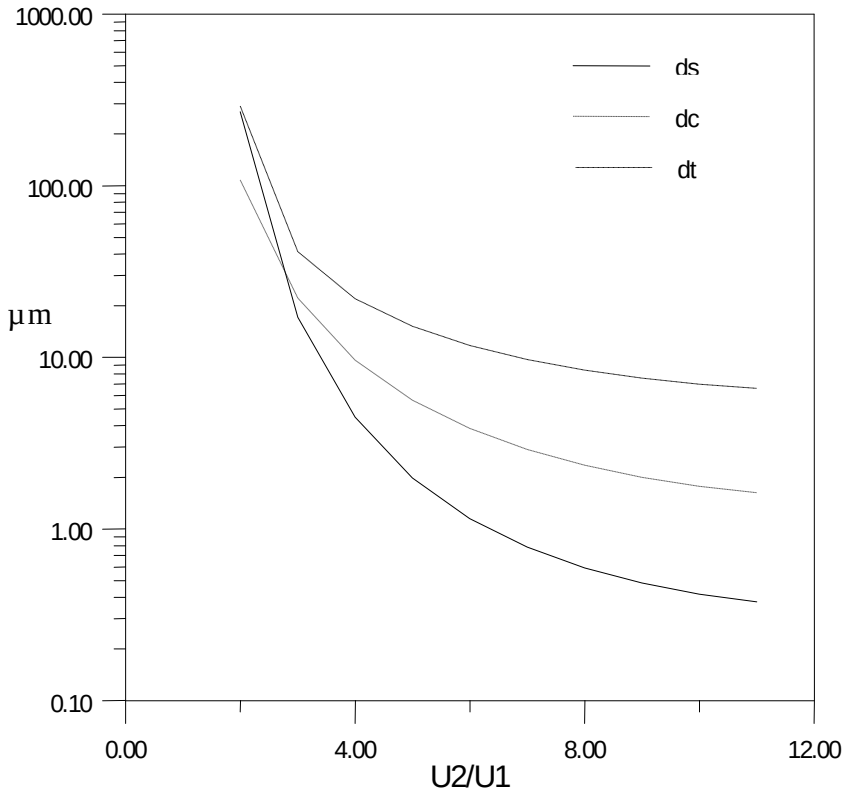

Figure 3-19 : The spherical, chromatic and total aberration disks of a three-electrode einzel lens as a functions of voltage ratio U2/U1 operated under zero magnification condition.

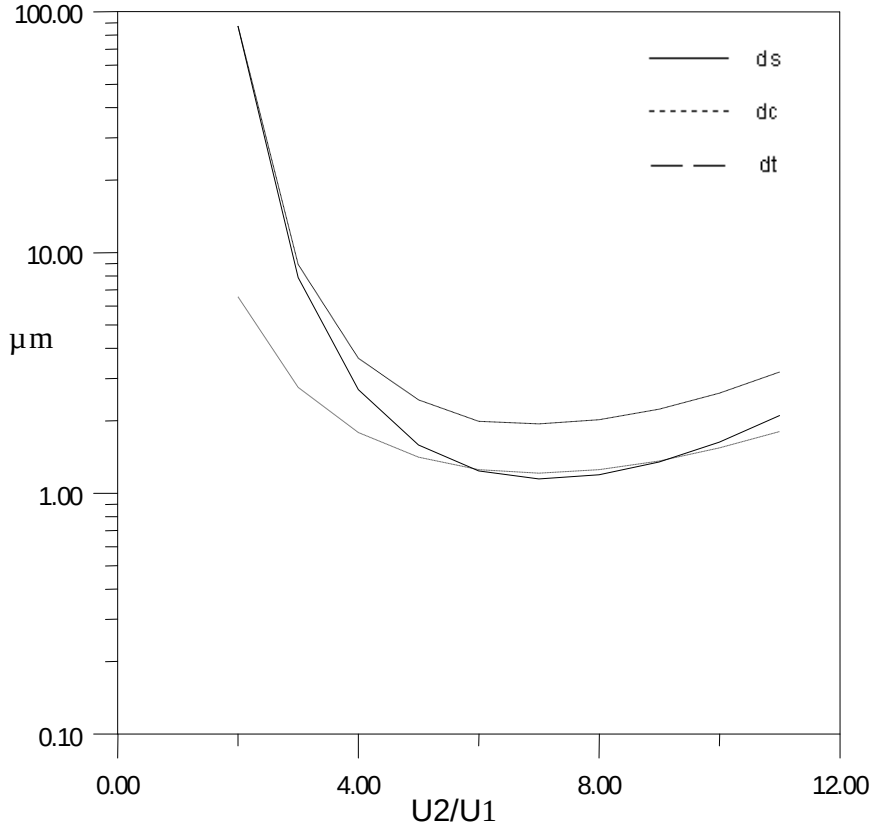

Figure 3-20 : The spherical, chromatic and total aberration disks of a three-electrode einzel lens as a functions of voltage ratio U2/U1 operated under infinite magnification condition.

3.4. Einzel Lens With Misalignment Effect

The behavior of the three electrodes einzel lens which they shift from the optical axis z due to misalignment effect which approximated by introducing a shift function $Us_L(z)$ given in equation (2-5) is shown in figure 3-21.

The beam trajectories for an einzel lens which including misalignment effect under zero and infinite magnification conditions are shown in figure 3-22a and 3-22b respectively.

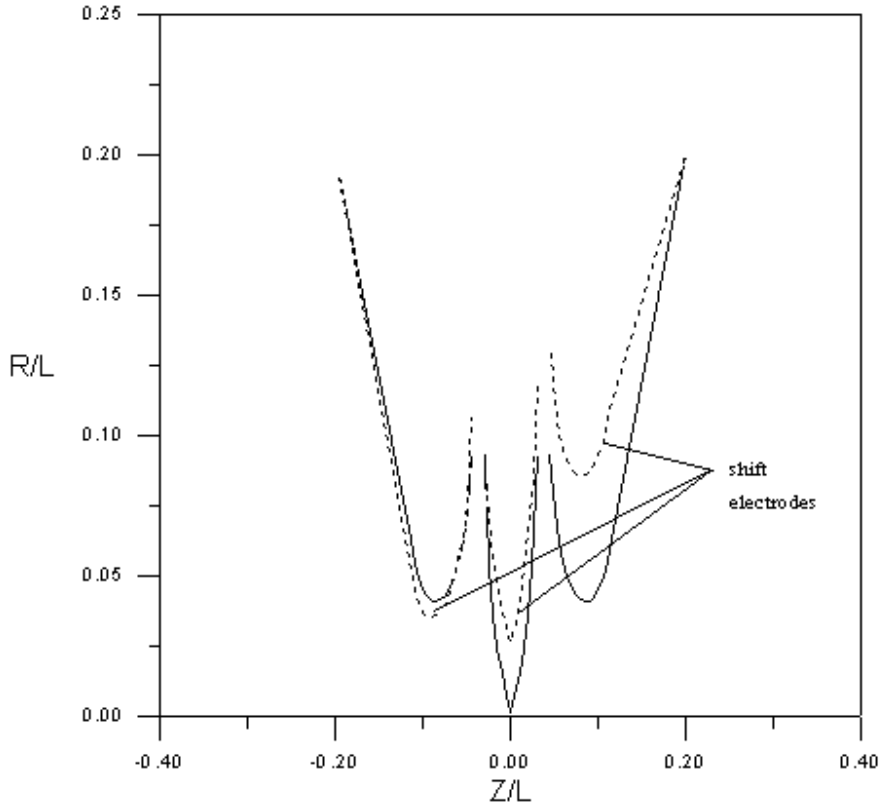

Figure 3-21 : The profile of the three electrode einzel lens with and without misalignment effect.

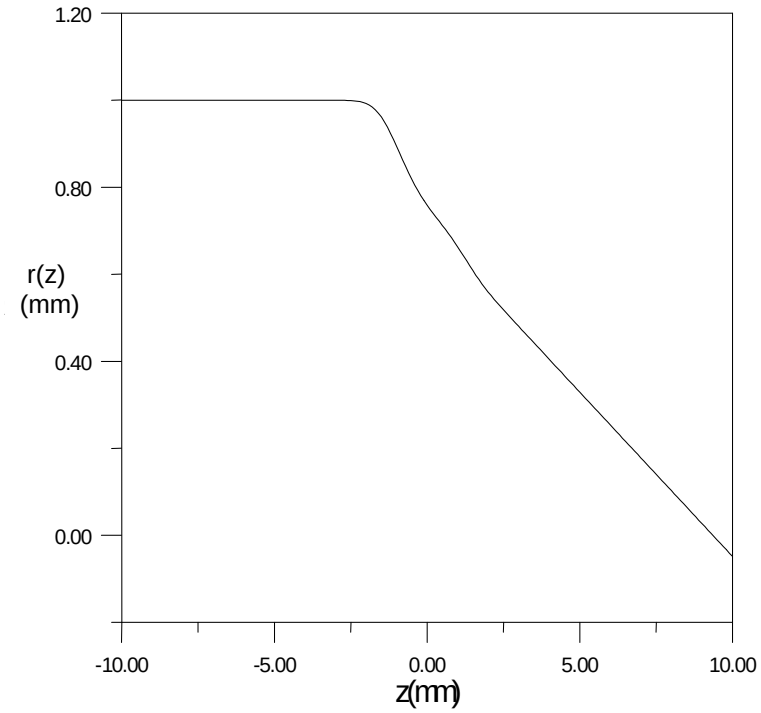

(a)

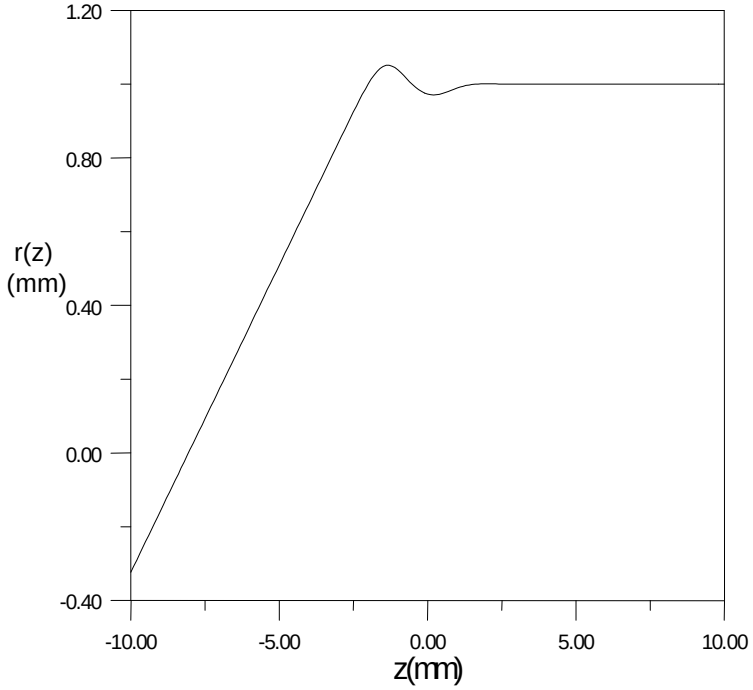

(b)

Figure 3-22 : The trajectory along the optical axis of an einzel lens which including misalignment effect under (a) Zero magnification condition and (b) Infinite magnification condition.

Figure 3-23a and 3-23b shows the variation of fi/L and fo/L under zero and infinite magnification conditions respectively with the voltage ratio U2/U1. It is seen that fi/L and fo/L decreases with increasing voltage ratio U2/U1, i.e. the lens become stronger or its refractive power become longer.

The relation between spherical, chromatic and total aberration disks d_s, d_c and d_t respectively for an einzel lens which including misalignment effect on a logarithmic scale with voltage ratio U2/U1 is shown in figures 3-24 and 3-25 .

Figure 3-24 shows the relation spherical, chromatic and total aberration disks d_s, d_c and d_t respectively with U2/U1 under zero magnification condition. It is clear that the spherical and chromatic aberration disks increases as U2/U1 increases. The d_s and d_c become equal and have a values of 0.95µm and 42.2µm at U2/U1=2.1 and 8.8 respectively. At U2/U1 <8, the d_t close to the d_c; but when U2/U1 exceeds 9 the d_s becomes dominant, approaching the value of d_t. The minimum values of spherical, chromatic and total aberration disk are 0.9 µm, 0.825µm and 1.22µm respectively at U2/U1=2.

Figure 3-25 shows the relation spherical, chromatic and total aberration disks d_s, d_c and d_t respectively with U2/U1 under infinite magnification condition. It is clear that the spherical and chromatic aberration disks increases with increasing voltage ratio U2/U1. The curves d_s and d_t coincide indicating that the value of spherical aberration disk d_s is always dominant. The minimum values of spherical, chromatic and total aberration disks are 1.09µm, 0.128µm and 1.097µm respectively at U2/U1=2.

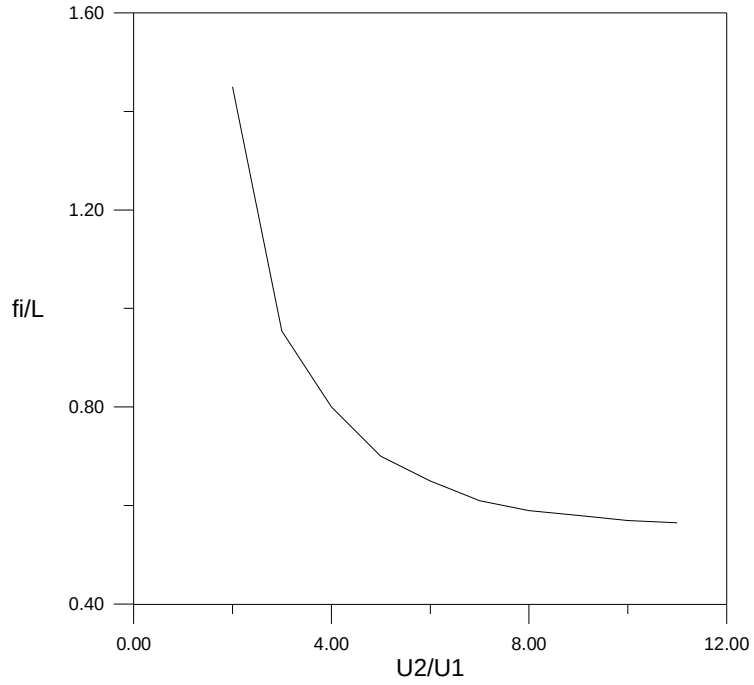

(a)

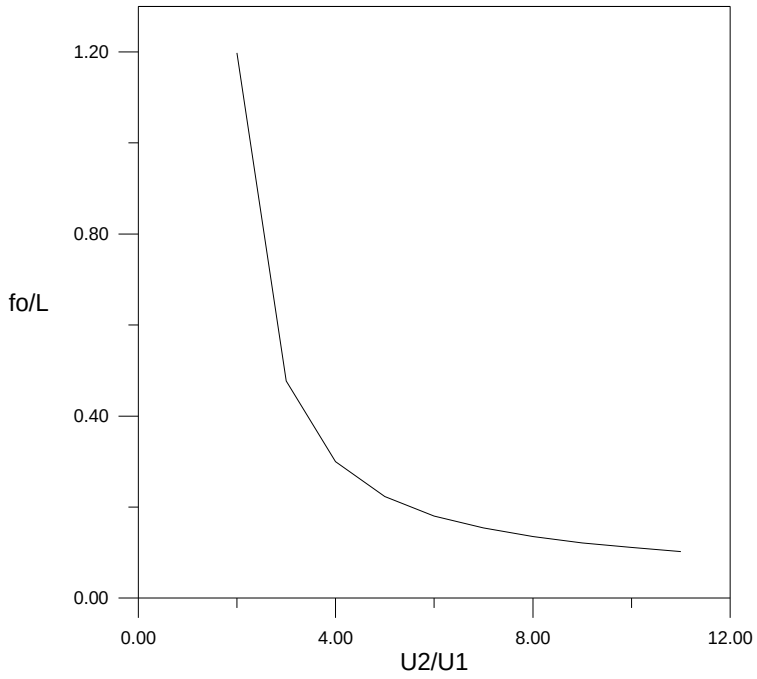

(b)

Figure 3-23 : The relative focal length of the three electrode einzel lens which including misalignment effect as a function of voltage ratio under (a) Zero magnification condition (b) Infinite magnification condition.

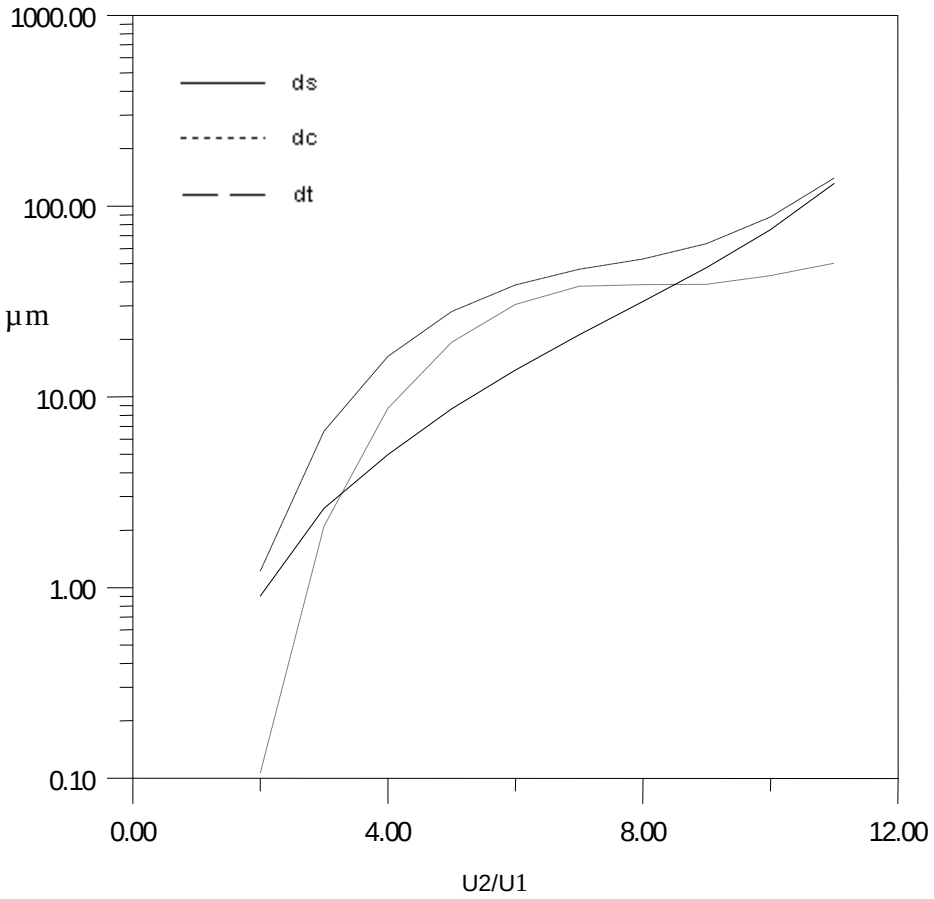

Figure 3-24 : The spherical, chromatic and total aberration disks of a three-electrode immersion lens which including misalignment effect as a functions of voltage ratio U2/U1 operated under zero magnification condition.

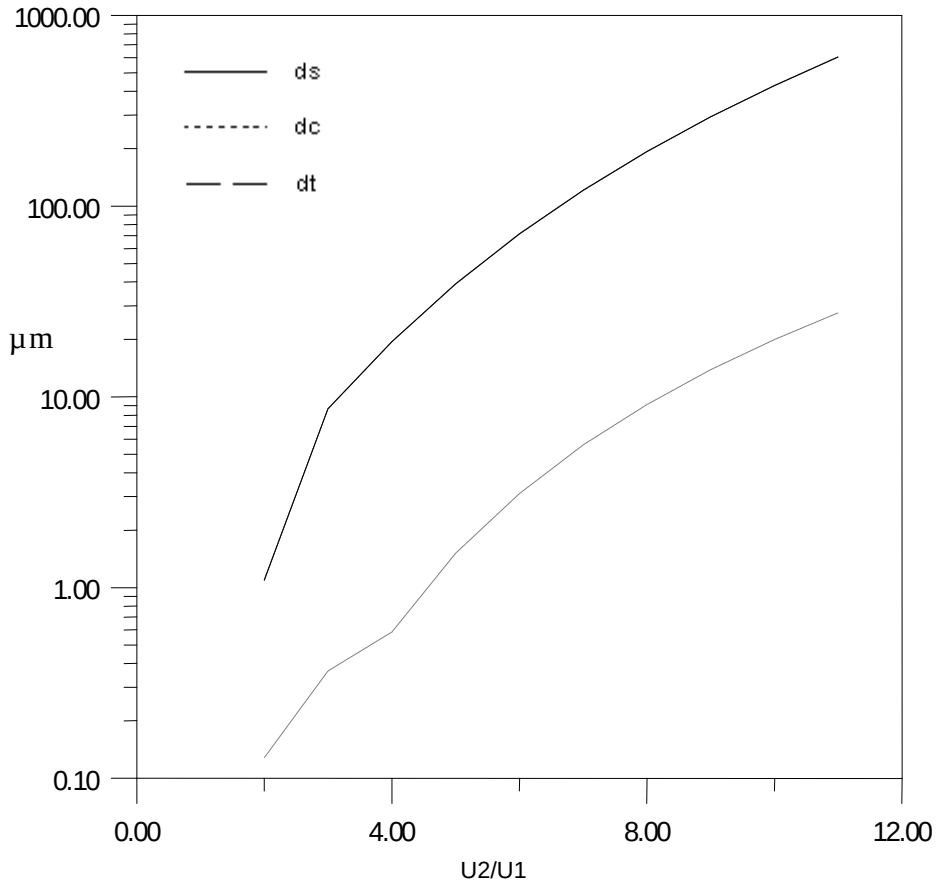

Figure 3-25 : The spherical, chromatic and total aberration disks of a three-electrode immersion lens which including misalignment effect as a functions of voltage ratio U2/U1 operated under infinite magnification condition.

4. CONCLUSIONS AND RECOMMENDATIONS FOR FUTURE WORK

4.1. *Conclusions*

It appears from the present investigation that it is possible to design various types of electrostatic lenses with small aberrations operated under different potential ratios and magnifications conditions. The two functions that have been put forward are to approximate the axial potential distribution introduced einzel and immersion electrostatic lenses.

It has been found that it is possible to design an einzel and immersion electrostatic lenses with small aberrations with the existence of misalignment effect operated under zero and infinite magnification conditions due to the choice of the proper function U_{SL}.

It has been shown that the aberration disk of electrostatic lens without misalignment effect decreases as voltage ratio U2/U1 increases, and it increases in electrostatic lens which including misalignment effect as voltage ratio U2/U1 increases.

4.2. *Future Work*

The following topics may be suggested for future work:

(a) An investigation on the design of a system of electrostatic lens and deflector due to misalignment effect as aberration correction.

(b) Design of a magnetic optical systems due to misalignment effect as aberration correction.

(c) Design of an electrostatic lens taking into account the space charged effect with misalignment effect.

Appendix

The spherical aberration disk due to misalignment effect in electrostatic lens reffered to object side is given by:

$$d_s = \frac{1}{\sqrt{U_o}\, r_o'} \int_{z_o}^{z_i} U r P_3 dz \tag{A-1}$$

where

$$P_3 = \frac{1}{\sqrt{U}} \frac{\partial}{\partial z}(r'\sqrt{U}Y) - (\frac{U''}{4U}(r - U_{SL}) + \frac{VF_1}{2U})Y + (\frac{U'''}{32U}(r - U_{SL})^3 + \frac{VF_1}{8U}(r - S_D)^2 + \frac{VF_1''}{16U}(r - S_D)^2 - \frac{3VF_3}{2U}(r - S_D)^2), \tag{A-2}$$

$$Y = \frac{U''}{8U}(r - U_{SL})^2 + (\frac{1}{4U}VF_1(r - S_D))^2 + \frac{1}{2}r'^2, \tag{A-3}$$

$$F_1(z) = \sum_{j=1}^{N} f_{1i}(z)\exp(ix_i),$$

$$F_3(z) = \sum_{j=1}^{N} f_{3i}(z)\exp(3ixi), \tag{A-4}$$

and

$$V = V_x + iV_y \tag{A-5}$$

$f_{1i}(z)$ and $f_{3i}(z)$ are the first and third harmonic field functions for the jth deflector, x_i is the rotation angle, and V_x and V_y are the x and y directional deflector voltages. In the present work the aberration due to misalignment in deflector is neglected, hence equation (A-2) and (A-3) are reduced to the following form:

$$P_3 = \frac{1}{\sqrt{U}} \frac{\partial}{\partial z}(r'\sqrt{U}Y) - (\frac{U''}{4U}(r - U_{SL}))Y + (\frac{U'''}{32U}(r - U_{SL})^3, \tag{A-6}$$

$$Y = \frac{U''}{8U}(r - U_{SL})^2 + \frac{1}{2}r'^2 \tag{A-7}$$

by substituting equation (A-7) in equation (A-6) one obtains:

$$P_3 = \frac{1}{\sqrt{U}}\frac{\partial}{\partial z}(r'\sqrt{U}(\frac{U''}{8U}(r-U_{SL})^2+\frac{1}{2}r'^2))-(\frac{U''}{4U}(r-U_{SL}))(\frac{U''}{8U}(r-U_{SL})^2+\frac{1}{2}r'^2)$$
$$+(\frac{U'''}{32U}(r-U_{SL})^3$$
$$=\frac{1}{\sqrt{U}}(\frac{1}{8}(r-U_{SL})^2(-\frac{1}{2}U^{-3/2}U''r'+U^{1/2}U''r''+U^{-1/2}U'''r')+(\frac{1}{4}U^{-1/2}U''r'(r-U_{SL})(r'-U'_{SL}))+$$
$$(\frac{1}{2}(\frac{1}{2}U^{-1/2}r'^2+3U^{1/2}r'^2r'')))-(\frac{U''}{4U}(r-U_{SL}))(\frac{U''}{4U}(r-U_{SL})^2+\frac{1}{2}r'^2)+(\frac{U'''}{32U}(r-U_{SL})^3) \quad \text{(A-8)}$$

let

$$C_1 = \frac{1}{8\sqrt{U}}(r-U_{SL}{}^2)(U^{-\frac{1}{2}}U''r'+U^{-\frac{1}{2}}U''r''-\frac{1}{2}U^{-\frac{3}{2}}U''r'),$$

$$C_2 = \frac{1}{\sqrt{U}}(\frac{1}{4}U^{\frac{1}{2}}U''r'(r-U_{SL})(r'-U'_{SL})+\frac{1}{2}(\frac{1}{2}U^{-\frac{1}{2}}r'^3+3U^{\frac{1}{2}}r'^2r'')),$$

$$C_3 = (\frac{U''}{4U}(r-U_{SL}))(\frac{U''}{8U}(r-U_{SL})^2+\frac{1}{2}r'^2)+(\frac{U'''}{32U}(r-U_{SL})^3) \quad \text{(A-9)}$$

then equation (A-8)becomes:

$$P_3 = C_1 + C_2 - C_3 \quad \text{(A-10)}$$

using equation (A-10) in equation (A-1) gives:

$$d_s = \frac{1}{\sqrt{U_o}r'_o}\int_{z_o}^{z_i}\sqrt{U}r(C_1+C_2-C_3)dz \quad \text{(A-11)}$$

Note: equation (A-11) can be calculated without using U''' and U''''.

References

Ahmad, A. K. (1993)

Computerized investigation on the optimum design and properties of the electrostatic lenses

Ph. D. Thesis, Al-Nahrain University, Baghdad, Iraq

Al-Ani, S. K. (1996)

A computational study of space-charge effect on the design of electrostatic lenses

Ph. D Thesis

Al-Nahrain University, Baghdad, Iraq

Al-Mudarris, F. A. J. (2001)

Computer-aided design of an ion –optical transport and focusing system

Ph. D. Thesis, Al-Nahrain University, Baghdad, Iraq

Baranova, L.A., and Read, F.H. (1999)

Minimization of the aberrations lens systems composed of quadrupole and actupole lenses

Int. J. Mass Spectrom, **189**, pp 19-26

Baranova, L.A., and Read, F.H. (2001)

Aberration caused by mechanical misalignment in electrostatic quadrupole lens systems

Optik, **112**, pp 131-138

Baranova, L.A., Read, F.H., and Cubric, D. (2004)
Computational simulation of an electrostatic aberration corrector for a low-voltage scanning electron microscope
Nucl. Instrum. Meth., **A519**, pp 42-48

El-Kareh, A. B., and El-Kareh, J. C. J, (1970)
Electron Beams, Lenses, and Optics
(Academic Press)

Glatzel, U. and Lenz, F. (1988)
Optimization of electrostatic immersion lenses
Optik, **79**, pp 15-18

Hawkes, P.W. (1967)
Lens aberration Focusing of Charged Particles, ed. **Septier, A.,** 411-468
(Academic Press, New York)

Hawkes, P.W. (1973)
Computer-aided design in electron optics
Computer Aided Design, **5**, pp 200-214

Hawkes, P.W. and Kasper, E. (1989)
Principles of Electron Optics vol. 1
(Academic Press: London)

Kiss, L. (1988)

Computerized investigation of electrostatic lens potential distribution

12th IMACS World Congress, ed. Vicherestsky, R. Paris(1988)

Kiss, L. (1989)

Electrostatic lens potentials with small relativistic spherical aberration

Rev. Sci. Instrum., **60**, pp 907-909

Kurihara, K. (1990)

Aberration due to misalignment in the electrostatic lens and deflection systems

J.Vac. Sci. Technol., **B8**, pp 452-455

Lawson, J. D. (1977)

The Physics of Charged-Particle Beams

(Clarendon Press: Oxford), pp 13-117

Moses, R.W. (1970)

Minimum aperture aberration of quadrupole lens system

Rev. Sci. Instrum., **41**, pp 729-740

Moses, R.W. (1971)

Minimum chromatic aberration of magnetic quadrupole objective lenses

Rev. Sci. Instrum., **42**, pp 828-831

Munro, E. (1975)

Design and optimization of magnetic lenses and deflection systems for electron beams

J. Vac. Sci. Technol., **12**, pp 1146-1151

Paszkowski, B. (1968)
Electron optics
(Iliffe Book: London)

Read, F. H. (1998)
Aberration due to localized potential defects (patch fields) on apertures
Rev. Sci. Instrum., **69**, pp 84-90

Scheinfein, M. and Galantai, A. (1986)
Multiobjective optimization techniques for design of electrostatic charged particle lenses
Optik, **74**, pp 154-164

Szep, J. and Szilagyi, M., (1987)
Statistical error analysis of electrode construction for electrostatic spline lenses
J. Appl. Phys., **62**, pp 3539-3542

Szep, J and Szilagyi, M., (1988)
A novel approach to the synthesis of electrostatic lenses with minimized aberrations
IEEE Transactions on Electron Devices, **35**, pp 1181-1183

Szilagyi, M. (1977a)
A new approach to electron optical optimization
Optik, **48**, pp 215-224

Szilagyi, M. (1977b)

A dynamic programming search for magnetic field distributions with minimum spherical aberration

Optik, **49**, pp 223-246

Szilagyi, M. (1984)

Reconstruction of electron and pole pieces from optimized axial field distribution of electron and ion optical systems

Appl. Phys. Lett., **45**, pp 499-501

Szilagyi, M. (1985)

Electron optical synthesis and optimization

Proc. IEEE **73,** pp 412-418

Szilagyi, M. (1987)

Electrostatic spline lenses

J.Vac. Sci. Technol., **A5**, pp 273-27**8**

Szilagyi, M. (1988)

Electron and Ion Optics

(Plenum Press: New York)

Szilagyi, M., Szep, J. and Lugosi, E. (1987)

A systematic analysis of two-electrode electrostatic lenses

IEEE Trans., **ED-34**, pp 1848-1857

Tsumagari (1986)

Aberrations of electrostatic systems with machining error

J. Vac. Sci. Technol., **B4 (1),** pp 140-142

Zhigarev, A. (1975)

Electron Optics and electron-beam devices

(Mir Publishers, Moscow)

Republic of Iraq
Ministry of Higher Education
and Scientific Research
AL-Nahrain University
College of Science

THE ABERRATION CORRECTION DUE TO MISALIGNMENT IN ELECTROSTATIC LENSES

A Thesis

Submitted to the College of Science of Al-Nahrain Univresity

in Partial Fulfillment of the Requirements for the Degree of Master of Science in Physics

by

Roaa Tahseen Abdullah Al-Sumaidaee
(B.Sc.in physics 2003)

in

Ramadan **1427 A.H.**
September **2006 A.D.**

بِسْمِ اللّهِ الرَّحْمَنِ الرَّحِيمِ

اقْرَأْ بِاسْمِ رَبِّكَ الَّذِي خَلَقَ (١) خَلَقَ الْإِنسَانَ مِنْ عَلَقٍ (٢) اقْرَأْ وَرَبُّكَ الْأَكْرَمُ (٣)الَّذِي عَلَّمَ بِالْقَلَمِ (٤) عَلَّمَ الْإِنسَانَ مَا لَمْ يَعْلَمْ (٥)

صَدَقَ اللّهُ الْعَظِيمِ

سورة العلق (١-٥)

Certification

We certify that this thesis entitled "**The Aberration Correction Due to Misalignment in Electrostatic Lenses**" is prepared by **Roaa Tahseen Abdullah Al-Sumaidaee** under our supervision at the College of Science of AL-Nahrain University in partial fulfillment of the requirements for the degree of **Master of Science** in Physics.

Signature:
Name: **Dr.Ahmad K. Ahmad**
(Supervisor)
Date / / 2006

In the view of the recommendations, I forward this thesis for debate by the examination committee.

Signature:
Name: **Dr. Ahmad K. Ahmad.**
(Head of physics department)
Date: */ / 2006*

Examination Committee Certification

We certify that we have read the thesis entitled **The Aberration Correction Due to Misalignment in Electrostatic Lenses**, and as Examining Committee, examined the student **Roaa Tahseen Abdullah Al-Sumaidaee** on its contents, and that in our opinion it is adequate for the partial fulfillment of the requirements for the degree of **Master** of **Science** in **Physics**.

Signature:
Name: **Dr.Ayad A.Al-Ani**
Title: **Assistant Professor**
(Chairman)
Date: / /2006

Signature:
Name: **Dr.Samir Khdhir Yassin Al-Ani**
Title: **Assistant Prfessor**
(Member)
Date: / /2006

Signature:
Name: **Dr.M.I.Sanduk**
Title: **Assistant Prfessor**
(Member)
Date: / /2006

Signature:
Name: **Dr. Ahmad K. Ahmad**
Title: **Assistant Professor**
(Supervisor)
Date: / /2006

Approved by the University Committee of Postgraduate studies

Signature:
Name: **Dr. Laith Abdul Aziz A.AL-Ani**
Title: **Assistant Professor**
(Dean of the College of Science)
Date: / / 2006

Dedicated
To
My Family
And Specially
To The Memory Of
My Father

Acknowledgement

I wish to extend my appreciation to my supervisor **Dr. Ahmad K. Ahmad** for supervising the present work and for his support and encouragement throuhout the research.

I am most greatfull to the Dean of College of Science and the staff of the Department of Physics at Al-Nahrain University, for their valuable support and cooperation.

Finally, I am most greatfull to my mother , my husband Hassan, my brothers Zaid and Ali, and my sister Noor for their patience and encouragement throughout this work.

Roaa

CHAPTER ONE

CHAPTER TWO

CHAPTER THREE

CHAPTER FOUR

APPENDIX

REFERENCES

جمهورية العراق
وزارة التعليم العالي والبحث العلمي
جامعة النهرين
كلية العلوم
قسم الفيزياء

تصحيح الزيغ بسبب عدم التراصف في العدسات الكهروسكونية

رسالة

مقدمة إلى كلية العلوم في جامعة النهرين
وهي جزء من متطلبات نيل درجة ماجستير علوم في الفيزياء

من قبل

رؤى تحسين عبد الله الصميدعي

(بكالوريوس علوم في الفيزياء ٢٠٠٣)

في

رمضان ١٤٢٧هـ
ايلول ٢٠٠٦ م

المستخلص

أجري بحث حاسوبي في مجال بصريات الجسيمات المشحونة. يهتم البحث بتصميم منظومات عدسات كهروسكونية بوجود وعدم وجود تأثير عدم التراصف تعمل تحت ظروف تكبير مختلفة.

أن توزيع مجال الجهد لعدسه أحادية الجهد وعدسة مغمورة كهروسكونية تم تمثيله بدوال تحليلية. تم حل معادلة الأشعة المحورية للمجالات المقترحة لإيجاد مسار الجسيمات المشحونة المارة في كل عدسة. ومن توزيع الجهد المحوري ومشتقتيه الأولى والثانية. تم حساب الخواص البصرية كالبعد البؤري والزيغين الكروي واللوني. كذلك تم إيجاد شكل أقطاب كل عدسة كهروسكونية ببعدين وبثلاثة أبعاد. ويعتمد الزيوغ في العدسات الكهروسكونية اعتماداً كبيراً على تراصف الاقطاب، وقد وجد انه عامل مهم يؤثر على الشكل الهندسي لمنظومة العدسة الكهروسكونية.

أن نتائج هذه الدراسة لا تبرهن نظريا" أمكانية تصميم منظومات عدسة كهروسكونية بزيوغ واطئة فحسب بل تبين إمكانية تصنيع مثل هذه العدسات عمليا".